



## HIMMELI v1.0: Helsinki Model of Methane build-up and emission for peatlands

Maarit Raivonen<sup>1</sup>, Sampo Smolander<sup>1,2</sup>, Leif Backman<sup>3</sup>, Jouni Susiluoto<sup>3</sup>, Tuula Aalto<sup>3</sup>, Tiina Markkanen<sup>3</sup>, Jarmo Mäkelä<sup>3</sup>, Janne Rinne<sup>4</sup>, Olli Peltola<sup>1</sup>, Mika Aurela<sup>3</sup>, Marin Tomasic<sup>1</sup>, Xuefei Li<sup>1</sup>,  
5 Tuula Larmola<sup>5</sup>, Sari Juutinen<sup>6</sup>, Eeva-Stiina Tuittila<sup>7</sup>, Martin Heimann<sup>1,8</sup>, Sanna Sevanto<sup>9</sup>, Thomas Kleinen<sup>10</sup>, Victor Brovkin<sup>10</sup>, Timo Vesala<sup>1,11</sup>

<sup>1</sup>Division of Atmospheric Sciences, Department of Physics, University of Helsinki, P.O.Box 68, 00014 Helsinki, Finland

<sup>2</sup>Princeton Environmental Institute, Guyot Hall, Princeton University, Princeton, NJ 08544, USA

<sup>3</sup>Climate research, Finnish Meteorological Institute, P.O. Box 503, 00101 Helsinki, Finland

10 <sup>4</sup>Department of Physical Geography and Ecosystem Science, Lund University, Sölvegatan 12, 22362 Lund, Sweden

<sup>5</sup>Natural Resources Institute Finland (Luke), Latokartanonkaari 9, 00790 Helsinki, Finland

<sup>6</sup>Department of Environmental Sciences, University of Helsinki, Viikinkaari 1, 00790 Helsinki, Finland

<sup>7</sup>School of Forest Sciences, University of Eastern Finland, P.O. Box 111, 80770 Joensuu, Finland

<sup>8</sup>Max Planck Institute for Biogeochemistry, 07745 Jena, Germany

15 <sup>9</sup>Earth and Environmental Sciences Division, Los Alamos National Laboratory, Bikini Atoll Rd. MS J535, Los Alamos, NM 87545, USA

<sup>10</sup>Max Planck Institute for Meteorology, Bundesstr. 53, 20146, Hamburg, Germany

<sup>11</sup>Department of Forest Sciences, University of Helsinki, P.O.Box 27, 00014 Helsinki, Finland

*Correspondence to:* Maarit Raivonen (maarit.raivonen@helsinki.fi)

20 **Abstract.** Wetlands are one of the most significant natural sources of methane (CH<sub>4</sub>) to the atmosphere. They emit CH<sub>4</sub> because decomposition of soil organic matter in waterlogged anoxic conditions produces CH<sub>4</sub>, in addition to carbon dioxide (CO<sub>2</sub>). Production of CH<sub>4</sub> and how much of it escapes to the atmosphere depend on a multitude of environmental drivers. Models simulating the processes leading to CH<sub>4</sub> emissions are thus needed for upscaling observations to estimate present CH<sub>4</sub> emissions and for producing scenarios of future atmospheric CH<sub>4</sub> concentrations. Aiming at a CH<sub>4</sub> model that can be added to  
25 models describing peatland carbon cycling, we developed a model called HIMMELI that describes CH<sub>4</sub> build-up in and emissions from peatland soils. It is not a full peatland carbon cycle model but it requires the rate of anoxic soil respiration as input. Driven by soil temperature, leaf area index (LAI) of aerenchymatous peatland vegetation and water table depth (WTD), it simulates the concentrations and transport of CH<sub>4</sub>, CO<sub>2</sub> and oxygen (O<sub>2</sub>) in a layered one-dimensional peat column. Here, we present the HIMMELI model structure, results of tests on the model sensitivity to the input data and to the description of  
30 the peat column (peat depth and layer thickness), and an intercomparison of the modelled and measured CH<sub>4</sub> fluxes at Siikaneva, a peatland flux measurement site in Southern Finland. As HIMMELI describes only the CH<sub>4</sub>-related processes, not the full carbon cycle, our analysis revealed mechanisms and dependencies that may remain hidden when testing CH<sub>4</sub> models connected to complete peatland carbon models, which is usually the case. Our results indicated that 1) the model is flexible and robust and thus suitable for different environments; 2) the simulated CH<sub>4</sub> emissions largely depend on the prescribed rate  
35 of anoxic respiration; 3) the sensitivity of the total CH<sub>4</sub> emission to other input variables, LAI and WTD, is mainly mediated



via the O<sub>2</sub> concentrations that affect the CH<sub>4</sub> production and oxidation rates; 4) with given input respiration, the peat column description does not affect significantly the simulated CH<sub>4</sub> emissions.

## 1 Introduction

Methane (CH<sub>4</sub>) is an important greenhouse gas, atmospheric concentrations of which have increased by more than 250% since  
5 preindustrial times, inducing the second largest radiative forcing (Myhre et al., 2013). Wetlands are the largest single natural  
CH<sub>4</sub> source to the atmosphere and their CH<sub>4</sub> emissions respond to changes in climatic conditions, which can be seen at global  
level (Bridgman et al., 2013; Turetsky et al., 2014). In order to upscale observed CH<sub>4</sub> fluxes and to produce realistic scenarios  
for the future atmospheric greenhouse gas concentrations, it is thus essential to know how wetland CH<sub>4</sub> emissions respond to  
climatic variables. Modelling these responses has been active in recent years (e.g. Wania et al., 2010; Riley et al., 2011; Melton  
10 et al., 2013; Schuldt et al., 2013; Grant et al., 2015).

Freshwater wetlands emit CH<sub>4</sub> from decomposition of soil organic matter because oxygen (O<sub>2</sub>) concentrations in their water-  
saturated soils are low and no alternative electron acceptors exist. Anoxic decomposition of soil organic matter is partly carried  
out by methanogenic microbes that produce CH<sub>4</sub>, so the decomposition process releases both CH<sub>4</sub> and carbon dioxide (CO<sub>2</sub>)  
15 (Nilsson and Öquist, 2009). Anoxia has also forced vascular wetland plants to develop techniques to get O<sub>2</sub> to their roots that  
extend to the inundated soil layers. For example, sedge species from genera *Carex* and *Eriophorum*, common in northern fen-  
type peatlands, have aerenchyma, special tissue with air-filled spaces that allows diffusion of O<sub>2</sub> from the atmosphere to the  
roots (Moog and Brüggemann, 1998). Some aquatic plants transport O<sub>2</sub> actively through the aerenchyma with pressurized  
through-flow (Brix et al., 1996). As a by-product, these mechanisms also transport CH<sub>4</sub> to the atmosphere (Morrissey et al.,  
20 1993; Brix et al. 1996). In addition to transfer via plants, CH<sub>4</sub> is known to be emitted from peatlands as ebullition, i.e. release  
of CH<sub>4</sub> bubbles into the atmosphere, and by diffusion through the peat column. CH<sub>4</sub> can also be consumed in the soil by  
methanotrophic bacteria that derive their energy by oxidizing CH<sub>4</sub> to CO<sub>2</sub>.

The three transport mechanisms and the CH<sub>4</sub> oxidation have been implemented in many peatland models in which the peat  
25 column is divided into layers and physically based formulations simulate the carbon processes in them (see a review in Xu et  
al. 2016). Many of them have features adopted from previous models – for instance, the Walter and Heimann (1996, 2000)  
model of CH<sub>4</sub> production and emission is frequently utilized — but often the implementations include specific modifications.  
Some of the models also simulate the O<sub>2</sub> transport and the simulated O<sub>2</sub> concentrations affect the CH<sub>4</sub> processes. This type of  
models have been used in multiple studies (e.g., Berrittella and van Huissteden, 2009, 2011; Khvorostianov et al., 2008;  
30 Ringeval et al., 2011; Melton et al., 2013; Budishchev et al., 2014; Cresto Aleina et al., 2015; Grant et al., 2015), and some  
are referred to in the Assessment Report of the Intergovernmental Panel on Climate Change (IPCC; Ciais et al., 2013). These  
models have different approaches in simulating the production of CH<sub>4</sub>, ranging from separating distinct heterotrophic microbial



communities (Grant and Roulet, 2002) to taking a constant fraction of the simulated heterotrophic soil respiration (Riley et al., 2011). After that, the transport models essentially take care of determining which portion of the CH<sub>4</sub> is oxidized, and which is released to the atmosphere.

- 5 All existing soil carbon models do not yet include the simulation of peatland CH<sub>4</sub> emissions. As CH<sub>4</sub> transport and oxidation can be simulated separately from other soil carbon processes, without the need to feed back to the main soil model, they can form a separate module. For this purpose, we developed HIMMELI, Helsinki Model of MEthane buiLd-up and emIssion. It takes the rate of anoxic peat respiration as input, defined here as the rate of anoxic decomposition of organic compounds in peatland soil, and computes the subsequent CH<sub>4</sub> emission by simulating the transport and build-up of CH<sub>4</sub>, O<sub>2</sub> and CO<sub>2</sub> in the
- 10 soil, as well as the CH<sub>4</sub> oxidation rate that depends on the prevailing O<sub>2</sub> concentrations. HIMMELI is driven with soil temperature, water table depth and the leaf area index of the gas-transporting plant canopy. It uses process descriptions largely adopted from earlier models, but the novelty is that it has been developed independent of a full peatland carbon model, with the ambition to obtain a robust and flexible model that can be easily used as a tool within different environments. Sensitivity analyses on the complete peatland models have been presented, mostly concentrating on the sensitivity to model parameters
- 15 (e.g. Berrittella and Huissteden, 2009, 2011; Tang et al. 2010; Wania et al., 2010; Zhu et al., 2014), but we are not aware of any studies which would have analyzed the sensitivity of the CH<sub>4</sub> models as such to driving variables. This kind of analysis is, however, important because a CH<sub>4</sub> module can form a considerable part of a peatland carbon model and studying it alone may reveal dependencies that affect the output CH<sub>4</sub> emissions but are not seen in sensitivity tests on full carbon models.
- 20 In the present work, we a) define key factors for CH<sub>4</sub> transport and oxidation, b) describe the model, c) analyze its dynamics and sensitivity of output fluxes to input data in steady-state tests, d) analyze the model sensitivity to the description of the peat column by running the model for a Finnish peatland flux measurement site Siikaneva (Rinne et al., 2007), and e) evaluate the model against measured CH<sub>4</sub> fluxes at Siikaneva.

## 2 Key factors for CH<sub>4</sub> transport and oxidation

- 25 The rate of CH<sub>4</sub> production in peat has been found to be controlled by peat and substrate quality, temperature and pH (Valentine et al., 1994; Bergman et al., 1999; Reiche, 2010). However, the final emissions depend on how much CH<sub>4</sub> is consumed by methanotrophic bacteria. This can be up to 100% of the CH<sub>4</sub> produced (Whalen, 2005; Fritz et al., 2011). The probability of a CH<sub>4</sub> molecule to get oxidized is thought to depend on which pathway it takes to escape from the soil since the conditions are suitable for methanotrophy mostly in oxic peat layers. Ebullition may bypass this oxidative zone (Coulthard et al., 2009) and
- 30 although methanotrophs are also found in some wetland plant roots (King, 1994), oxidation can largely be avoided by moving through the plants. Several studies have shown that the CH<sub>4</sub> emissions decrease clearly when the gas-transporting plants are



removed from a site, indicating that aerenchymatous vegetation is an effective transport route for CH<sub>4</sub> (Waddington et al., 1996; King et al., 1998; Green and Baird, 2012).

- Roots of sedges, particularly those of *Carex* species, extend deep to the soil (Shaver and Cutler, 1979; Saarinen, 1996). Therefore they have a large contact surface with the anoxic peat. The area of root surface permeable to gases was the most important factor controlling the CH<sub>4</sub> flux in *Juncus effusus*, another aerenchymatous species, and this permeable surface is concentrated in fine roots and the tips of coarser roots (Hennenberg et al., 2012). According to Reid et al. (2015), the rate for root-mediated gas transport in *P. australis* and *Spartina patens* increased during the growing season, indicating increase of permeable root surface area or aerenchyma along the summer. Thus, the growth of the plants seems to affect their gas transport capacity. Isotopic studies have shown that passive diffusion down the concentration gradient dominates the CH<sub>4</sub> transport in sedges (Chanton and Whiting, 1993; Popp et al., 1999), and Moog and Brüggemann (1998) also demonstrated that diffusion is a sufficient explanation for the supply of O<sub>2</sub> to the roots of *Carex* species. There are, however, contrasting findings about where the main resistance for the diffusive CH<sub>4</sub> flux lies. Kelker and Chanton (1997) suggested it is belowground, at the soil-root or root-shoot boundary, and that *Carex* releases CH<sub>4</sub> not through the leaf blades (and stomata) but from the point where the leaves bundle. This would be similar to rice (*Oryza sativa*), *Menyanthes trifoliata* and *J. effusus* that release CH<sub>4</sub> from the stem or leaf sheath, possibly through micropores, not stomata (Nouchi et al., 1990; Macdonald et al., 1998; Hennenberg et al., 2012). However, in the studies by Schimel (1995) and Morrissey et al. (1993), CH<sub>4</sub> seemed to exit the sedges through the leaf blades and stomata and this would thus form the main resistance for the flux in the plant. Diurnal variation of the CH<sub>4</sub> emissions could indicate stomatal control but clear diurnal patterns have not been observed (Rinne et al., 2007; Jackowicz-Korczyński et al., 2010), the maximum emissions may even occur at night (Mikkilä et al., 1995; Waddington et al., 1996; Juutinen et al., 2004). On the other hand, possible diurnal changes in O<sub>2</sub> diffusion to the rhizosphere may be reflected in the CH<sub>4</sub> fluxes since O<sub>2</sub> concentration affects the rate of CH<sub>4</sub> oxidation (Thomas et al., 1996), as well as diurnal changes in the CH<sub>4</sub> substrate input from the photosynthesizing vegetation may affect CH<sub>4</sub> production (Mikkilä et al., 1995).
- Gas ebullition occurs, in principle, when the concentration of a dissolved gas reaches saturation, but in practice, CH<sub>4</sub> ebullition has been observed in wetlands already with concentrations below saturation (Baird et al., 2004; Kellner et al., 2006; Waddington et al., 2009; Bon et al., 2014). Other gases increase the gas pressure and soil particles and impurities lower the energy barrier for gas nucleation. The CH<sub>4</sub> content in ebullitive gas fluxes has been estimated to be 45...60% (Glaser et al., 2004; Tokida et al., 2005; Kellner et al., 2006) and the rest consists mainly of O<sub>2</sub>, CO<sub>2</sub> and nitrogen (N<sub>2</sub>) (Tokida et al., 2005).
- The volumetric gas content (VGC) in the peat has been observed to be approximately 10...15% (Kellner et al., 2006; Tokida et al., 2007; Waddington et al., 2009) indicating that all the formed gas does not escape the soil. Ebullition events seem to be affected by atmospheric pressure. When the pressure declines, bubble volume increases and the solubility of gases decreases allowing more gases to accumulate in the bubbles, consequently, their buoyancy may overcome the forces that resist their movement and ebullition occurs (Tokida et al., 2007; Waddington et al., 2009). Increasing pressure, by contrast, may enhance



the bubble mobility through the peat by causing bubble size to decrease (Comas et al., 2011). Movement of bubbles also depends on the peat structure that varies along the peat column: the shallow, less decomposed peat has more space for the bubbles, while the more decomposed deeper peat layers are tighter packed (Comas et al., 2011).

- 5 Properties of the peat column also affect the diffusion of  $\text{CH}_4$  and  $\text{O}_2$  in the air- and water-filled peat pores. Porosity of the soil, i.e., the fraction of the soil volume that is taken up by the pore space, determines the rate of diffusion; the lower it is, the slower is diffusion. Different descriptions of the dependency of diffusion coefficient on the soil porosity or tortuosity have been presented (Millington, 1959; Collin and Rasmuson, 1988; Staunton, 2008). The porosity of peat soils is generally high, at least 80% (Mitsch and Gosselink, 2007). Therefore, peat does not hinder the diffusion as much as many other soil types. In
- 10 models the peat column is commonly considered in a simplified way, assuming that the water table depth (WTD) forms a border below which the peat is saturated with water and above which peat pores are air-filled. However, in reality the division is not this strict as VGC can be a considerable fraction of the total volume below the WTD for instance, due to the gas production in the peat (Waddington et al., 2009), and the peat can be wet above the WTD if the peat pores retain water when the WTD drops (Estop-Aragonés et al., 2012; Fan et al., 2014). Diffusion through the peat column is thought to be a minor
- 15 component in the total  $\text{CH}_4$  emissions of a peatland when gas-transporting vegetation is present at the site (Walter et al., 1996; Lai, 2009), because the diffusion coefficient in water is approximately 4 orders of magnitude lower than in gas (Staunton, 2008) and because the probability of  $\text{CH}_4$  being consumed by methanotrophs is higher in the peat, especially when the WTD is low (Estop-Aragonés et al., 2012).
- 20 Methanotrophic bacteria occur in all soils, not only wetlands, and methanotrophy in upland soils is the largest biogenic sink of atmospheric  $\text{CH}_4$  (Ciais et al., 2013). Rate of the  $\text{CH}_4$  oxidation reaction depends on the concentrations of both  $\text{CH}_4$  and  $\text{O}_2$  (Watson et al., 1997) and since  $\text{CH}_4$  oxidation is a biochemical reaction, the rate is also limited by factors that affect the microbial activity, such as temperature (Whalen and Reeburgh, 1996). When the WTD is low, the  $\text{O}_2$  concentrations in the top peat layers are high favoring  $\text{CH}_4$  oxidation (Moore et al., 2011; Estop-Aragonés et al., 2012). However, there can be anoxic
- 25 areas above the WTD (Silins and Rothwell, 1999; Fan et al., 2014) and the  $\text{O}_2$  transported down by plant roots provides conditions suitable for methanotrophy also in the inundated peat layers (Fritz et al., 2011).

### 3 Model and methods

#### 3.1 Model description

##### 3.1.1 General

- 30 The model (Fig. 1) simulates microbial and transport processes that take place in a one-dimensional peat column, keeping track on the concentration profiles of  $\text{CH}_4$ ,  $\text{O}_2$  and  $\text{CO}_2$ . The output is fluxes of  $\text{CH}_4$ ,  $\text{O}_2$  and  $\text{CO}_2$  between the soil and the



atmosphere, with the possibility to separate the contributions of the three different transport routes, as well as to extract the amount of oxidized CH<sub>4</sub>. The required input and the model output is explained in more detail within the model code package that is provided as a Supplement of this article.

5 The model is driven with:

- peat temperature, T (K)
- leaf area index of aerenchymatous gas-transporting vegetation, LAI (m<sup>2</sup> m<sup>-2</sup>)
- water table depth, WTD (m)
- anaerobic carbon decomposition rate, i.e., the rate of anoxic respiration for the area of the peatland,  $V_{anR}$  (mol m<sup>-2</sup> s<sup>-1</sup>).

10

Parameter values used in the present study are listed in Table 1. Some of them were taken directly from earlier literature (Arah and Stephen, 1998; Vile et al., 2005), but a set of parameter values was obtained by optimizing with Bayesian methods with respect to fluxes measured at the Siikaneva peatland site (see Sect. 3.3) using a least-squares objective function with the adaptive Metropolis Markov chain Monte Carlo method (Haario et al., 2001). The values used are the best estimate of these values, i.e., the parameter set of the lowest negative log-likelihood. The uncertainty of some of these parameters is rather high, and a more complete analysis can be found in Susiluoto et al. (2017, *in prep.*).

15

The reaction-diffusion equations governing the concentrations of the three compounds CH<sub>4</sub>, O<sub>2</sub> and CO<sub>2</sub> at depth  $z$  are (Eq. 1-3):

20

$$\frac{\partial}{\partial t} C_{CH_4}(t, z) = -\frac{\partial}{\partial z} F_{CH_4} - Q_{plt, CH_4} - Q_{ebu, CH_4} + R_{CH_4} - R_O \quad (1)$$

$$\frac{\partial}{\partial t} C_{O_2}(t, z) = -\frac{\partial}{\partial z} F_{O_2} - Q_{plt, O_2} - Q_{ebu, O_2} - R_{aR} - 2R_O \quad (2)$$

$$\frac{\partial}{\partial t} C_{CO_2}(t, z) = -\frac{\partial}{\partial z} F_{CO_2} - Q_{plt, CO_2} - Q_{ebu, CO_2} + (R_{anR} - R_{CH_4}) + R_O + R_{aR} \quad (3)$$

Here,  $F_{CH_4}$ ,  $F_{O_2}$ , and  $F_{CO_2}$  are the diffusive fluxes in the peat,  $Q_{plt, X}$  and  $Q_{ebu, X}$  are the transport rates of gas  $X$  between peat and atmosphere via plant roots and by ebullition, respectively,  $R_{CH_4}$  is CH<sub>4</sub> production rate,  $R_{anR}$  is the rate of anaerobic respiration,  $R_{aR}$  is the rate of aerobic respiration and  $R_O$  is the CH<sub>4</sub> oxidation rate.

25

The current set-up of the model runs in one-day resolution, taking the input as daily averages. The differential equations are solved simultaneously using the fourth order Runge-Kutta method. The internal time step is determined by the turnover time of CH<sub>4</sub> and O<sub>2</sub> concentrations in the peat. It is assumed that the longest usable time step is half of the turnover time.

30



### 3.1.2 Peat geometry, root distribution and movement of water

The model basically describes a one-dimensional vertically layered peat column. Peat depth and layer thicknesses are not fixed but different set-ups can be used. The only limitation for the layer structure is that if the peat thickness exceeds 2 m, there has to be a layer border exactly at the 2 m depth, because of how the roots are treated in the model. The layering below 2 m must start from that depth.

WTD is a strict divider of the peat into water-filled and air-filled parts. This has been implemented by adding an extra layer in the pre-described layer composition (Fig. 1). Its thickness is adjusted so that the water surface is always exactly at the interface between the two layers. This approach enables using the exact given WTD as input. Only in the case that the boundary of the extra layer would be closer than 1 cm to a boundary of the background layering, the WTD is rounded to this nearest permanent layer boundary. The water level can also be above the peat surface and in this case the extra layer is located above the peat surface.

Changing WTD essentially means addition or removal of water to/from the peat column. At the same time, the masses of CH<sub>4</sub>, O<sub>2</sub> and CO<sub>2</sub> need to be conserved. In the case of rising WTD, the CH<sub>4</sub>, O<sub>2</sub> and CO<sub>2</sub> that were in the air-filled layers are dissolved in the water until the concentrations in the newly water-filled layers reach the solubility limit with the previous air concentrations. The excess gas is pushed upwards to the lowest air-filled layer (or to the atmosphere). In the case of lowering WTD, the CH<sub>4</sub>, O<sub>2</sub> and CO<sub>2</sub> of the previously water-filled layers are introduced into the air-filled layers replacing them. This can cause abnormally high or low fluxes and concentrations in some layers, but these even out fast in relation to the daily time step, mainly through diffusion.

An essential role is played by the vertical distribution of plant roots since that determines how the input anoxic respiration and the gas-transporting root mass is distributed vertically. The formulation has been adopted from Wania et al. (2010):

$$f_{root}(z) = C e^{-z/\lambda} \quad (4)$$

where  $f_{root}(z)$  is the fraction of roots at depth  $z$ ,  $\lambda$  is a root depth distribution decay parameter and  $C$  is a normalizing constant defined so that the sum of root fractions equals 1 (Eq. 5):

$$\int_0^{z_{max}} f_{root}(z) dz = 1. \quad (5)$$

The maximum depth that the roots are assumed to reach is 2 m (Saarinen, 1996). If the peat depth exceeds 2 m there is a rootless zone at the bottom. The value of  $C$  depends on the peat thickness and geometry of the current peat column and it is calculated at each time step, so the root distribution can adjust to changing peat depth.



### 3.1.3 CH<sub>4</sub> production

Since root exudates are an important carbon source for the methanogens, the input anaerobic respiration ( $V_{anR}$ ) is distributed vertically along the root distribution in the anaerobic peat layers below the WTD (Eq. 6):

$$R_{anR}(z) = \frac{V_{anR}}{dz} f_{root,an}(z). \quad (6)$$

- 5 Here  $R_{anR}(z)$  (mol m<sup>-3</sup> s<sup>-1</sup>) is the rate of anoxic respiration at depth  $z$ ,  $f_{root,an}(z)$  refers to the ratio of root mass at depth  $z$  to the total root mass of the anaerobic zone and  $dz$  (m) is the layer thickness. CH<sub>4</sub> production rate  $R_{CH_4}$  (mol m<sup>-3</sup> s<sup>-1</sup>) in a peat layer at depth  $z$  is calculated as a fixed fraction ( $f_m$ ) of  $R_{anR}$  but the rate may be inhibited by dissolved O<sub>2</sub>, following Arah and Stephen (1998) (Eq. 7):

$$R_{CH_4}(z) = f_m R_{anR}(z) \frac{1}{1 + \eta C_{O_2}(z)}, \quad (7)$$

- 10 where  $\eta$  is a parameter reflecting the sensitivity of methanogenesis to O<sub>2</sub> inhibition. The CH<sub>4</sub> production rate in conditions with no O<sub>2</sub>, i.e.,  $C_{O_2}$  is zero, is called potential methane production (PMP) in this paper. The rest of the anaerobic respiration ( $R_{anR} - R_{CH_4}$ ) produces CO<sub>2</sub>.

- In the case that peat depth exceeds the maximum rooting depth 2 m, the model calculates what would be the anaerobic  
 15 respiration rate at the bottom root layer if all the input carbon was allocated in the rooting zone, then allocates 50% of that in the rootless layers, and the remainder is re-distributed to the rooting zone.

### 3.1.4 Aerobic respiration

All the O<sub>2</sub> in the peat is not consumed by the methanotrophs but other aerobic microbe processes like aerobic peat respiration also require O<sub>2</sub>. This O<sub>2</sub> consumption rate that affects the O<sub>2</sub> availability of CH<sub>4</sub> oxidation is estimated with a Michaelis-

- 20 Menten model, following Arah and Stephen (1998) (Eq. 8):

$$R_{aR}(z, T) = V_R(T) \frac{C_{O_2}(z)}{K_R + C_{O_2}(z)}, \quad (8)$$

where  $R_{aR}$  (mol m<sup>-3</sup> s<sup>-1</sup>) is the rate of aerobic respiration at temperature  $T$  at depth  $z$ ,  $V_R$  (mol m<sup>-3</sup> s<sup>-1</sup>) is the potential rate of respiration at temperature  $T$ , and  $K_R$  (mol m<sup>-3</sup>) is the Michaelis constant for the reaction. This reaction produces 1 mol of CO<sub>2</sub> per each mol of O<sub>2</sub> consumed.

### 25 3.1.5 CH<sub>4</sub> oxidation

Rate of CH<sub>4</sub> oxidation is assumed to follow the dual-substrate Michaelis-Menten kinetics (Arah and Stephen 1998) (Eq. 9):

$$R_O(z, T) = V_O(T) \frac{C_{O_2}(z)}{K_{O_2} + C_{O_2}(z)} \times \frac{C_{CH_4}(z)}{K_{CH_4} + C_{CH_4}(z)}, \quad (9)$$



where  $R_O$  ( $\text{mol m}^{-3} \text{s}^{-1}$ ) is the oxidation rate at temperature  $T$  at depth  $z$ ,  $V_O$  ( $\text{mol m}^{-3} \text{s}^{-1}$ ) is the potential oxidation rate at temperature  $T$ ,  $K_{O_2}$  ( $\text{mol m}^{-3}$ ) and  $K_{CH_4}$  ( $\text{mol m}^{-3}$ ) are the Michaelis constants for  $O_2$  and  $CH_4$ , respectively. Each  $CH_4$  mol oxidized consumes 2 moles of  $O_2$  and produces 1 mol  $CO_2$ .

### 3.1.6 Temperature dependency of microbial reactions

- 5 The reaction rates of oxidation and aerobic respiration depend on temperature following the form of the Arrhenius equation (Eq. 10):

$$V(T) = V_\emptyset \exp\left(\frac{\Delta E}{R} \left(\frac{1}{T_\emptyset} - \frac{1}{T}\right)\right), \quad (10)$$

where  $V(T)$  refers here to the rate of oxidation or aerobic respiration at temperature  $T$ ,  $V_\emptyset$  ( $\text{mol m}^{-3} \text{s}^{-1}$ ) is the reaction rate at the reference temperature  $T_\emptyset$  (K),  $R$  ( $\text{J mol}^{-1} \text{K}^{-1}$ ) is the gas constant and  $\Delta E$  ( $\text{J mol}^{-1}$ ) the activation energy of the reaction.

### 10 3.1.7 Ebullition

The ebullition model takes into account concentrations of  $CH_4$ ,  $CO_2$ ,  $O_2$  and  $N_2$  and uses the sum of their partial pressures to determine when ebullition occurs. This approach was used by Tang et al. (2010). In HIMMELI, ebullition is the only process that takes  $N_2$  into account. We assume  $N_2$  is always in equilibrium with the atmospheric concentration and so its partial pressure in the peat is always 78% of the atmospheric pressure. The model computes the solubilities of  $CH_4$ ,  $CO_2$  and  $O_2$  in water using the dimensionless Henry's law coefficient (see Appendix A for formulation; Sander, 2015).

If the sum of the partial pressures  $pp$  (Pa) of the dissolved  $CH_4$ ,  $CO_2$ ,  $O_2$  and  $N_2$  ( $pp_X$ ) exceeds the sum of the atmospheric and hydrostatic pressures ( $P_{atm}$  and  $P_{hyd}$ , respectively) (Eq. 11):

$$\sum_X pp_X(z) > P_{atm} + P_{hyd}(z) \quad (11)$$

- 20 ebullition occurs. The model first computes the fraction of ebullition,  $f_e$  (Eq. 12):

$$f_e(z) = \frac{\sum_X pp_X(z) - (P_{atm} + P_{hyd}(z))}{\sum_X pp_X(z)} \quad (12)$$

and this fraction of each gas is removed, expressed as a rate by introducing time constant  $k$  ( $\text{s}^{-1}$ ) in the equation. The value of  $k$  was chosen for numerical reasons to be  $1/1800$  s, which ensures the half-life of the gas is larger than the internal time step. The ebullition flux  $Q_{ebu,X}$  ( $\text{mol m}^{-3} \text{s}^{-1}$ ) of compound  $X$  from a soil layer at depth  $z$  thus is (Eq. 13):

$$25 \quad Q_{ebu,X}(z) = -k \frac{f_e(z) pp_X \sigma}{RT}, \quad (13)$$



where  $\sigma$  is peat porosity. Ebullition only occurs in the water-filled peat. If the WTD is below the peat surface, the ebullited gases are transferred into the lowest air-filled soil layer and they continue from there via diffusion in the peat or in plant roots. Otherwise the ebullition is released directly into the atmosphere.

### 3.1.8 Diffusion in the peat

- 5 Simulation of diffusion in the porous water-filled or air-filled peat takes into account the reduction in the diffusivity compared with pure water or air (see e.g. Iiyama and Hasegawa, 2005). The diffusion coefficients used in this study are listed in Appendix A. The effective diffusivities in the porous peat ( $D_{peat,w}$  and  $D_{peat,a}$ ;  $\text{m}^2 \text{s}^{-1}$ ) are calculated by multiplying the free-water or free-air diffusivities by (dimensionless) constant reduction factors  $f_{D,w}$  and  $f_{D,a}$ , whose values were derived from the optimization (Susiluoto et al., 2017) (Eq. 14 and 15).

$$10 \quad D_{peat,w} = f_{D,w} D_w \quad (14)$$

$$D_{peat,a} = f_{D,a} D_a \quad (15)$$

The diffusion ( $F_X$ ;  $\text{mol m}^{-2} \text{s}^{-1}$ ) of compound  $X$  between layers is calculated using a difference equation that is set up between the centre points ( $i-1$  and  $i$ ) of the layers (Eq. 16):

$$F_{i-1,i} = D_{peat,X} \frac{(C_{X,i-1} - C_{X,i})}{dx} \quad (16)$$

- 15 Here  $dx$  (m) is the distance between points  $i-1$  and  $i$  and  $C_{X,i-1}$  and  $C_{X,i}$  are the concentrations at these layers. The surface layer at the water-air interface is assumed to be in equilibrium with the gas phase concentrations according to the Henry's law. The diffusion flux across the water-air interface is then calculated from the difference in concentration between the layer centre points and water-air interface as shown by Bird et al. (1960). The final equation for the flux of compound  $X$  at the interface becomes (Eq. 17):

$$20 \quad F_X = \frac{2D_{peat,w,X}D_{peat,a,X}}{D_{peat,a,X} + D_{peat,w,X}k_{H,X}} \frac{C_{X,w} - k_{H,X}C_{X,a}}{dx}, \quad (17)$$

where  $D_{peat,w,X}$  and  $D_{peat,a,X}$  are the diffusion coefficients in the water and air-filled layers,  $k_{H,X}$  is the Henry's law coefficient in dimensionless form (Appendix A) and  $C_{X,w}$  and  $C_{X,a}$  ( $\text{mol m}^{-3}$ ) are the concentrations of compound  $X$  in the water-filled and air-filled layer, respectively.

### 3.1.9 Plant transport

- 25 Formulation of plant transport flux  $Q_{pl,X}$  of compound  $X$  ( $\text{mol m}^{-3} \text{s}^{-1}$ ) is similar to many other peatland models in that it describes diffusion in air-filled tubes that represent aerenchymatous plant roots. We employ the formulation from Stephen et al. (1998) that uses the density of cross-sectional area of root endings as the variable expressing the abundance of gas-transporting vegetation (Eq. 18):



$$Q_{plt,X}(z) = \frac{\varepsilon_r(z) D_{peat,a,X}}{\tau} \frac{C_X(z,t) - C_{atm,X}}{z} \quad (18)$$

Here  $\varepsilon_r$  is the density of cross-sectional area of root endings at depth  $z$  ( $\text{m}^2 \text{m}^{-3}$ ) and  $\tau$  is root tortuosity. To account for the porous structure of aerenchyma (Colmer, 2003), HIMMELI uses the same value as in air-filled peat,  $D_{peat,a}$  ( $\text{m}^2 \text{s}^{-1}$ ), as the diffusion coefficient inside roots. It is averaged over the temperatures of the different layers between each depth  $z$  that the roots go through.  $\varepsilon_r$  follows the root distribution and it depends on the LAI of the vegetation via (Eq. 19):

$$\varepsilon_r(z) = a_{mA} \frac{f_{root}(z) LAI}{A \times dz SLA}, \quad (19)$$

where  $a_{mA}$  expresses the cross-sectional area of root endings per root dry biomass ( $\text{m}^2 \text{kg}^{-1}$ ),  $A$  is the area of the peat layer ( $\text{m}^2$ ),  $dz$  is the layer thickness (m) and SLA is the specific leaf area ( $\text{m}^2 \text{kg}^{-1}$ ).

### 3.2 Model testing

We analyzed HIMMELI's sensitivity to the driving input variables and to the description of the peat column, i.e., peat column depth and layer thickness. The former was analyzed using steady-state tests and transition tests (see Section 3.2.1) and the latter by simulating the Siikaneva peatland site with different peat column descriptions (Section 3.2.2). In addition, we compared the modelled and measured  $\text{CH}_4$  fluxes at Siikaneva and conducted a rough evaluation of the model's ability to predict the observed  $\text{CH}_4$  emissions (Section 3.2.3).

#### 3.2.1 Testing model sensitivity to input data

The steady-state tests were conducted to study how sensitive the model is to the input data and to understand how the sensitivity depends on the modelled processes. We tested the model by running it into equilibrium with several different input value combinations, starting from empty concentration profiles of all the compounds. Specifically, we tested the sensitivity of the model to peat temperature, WTD, LAI (and corresponding root mass) and rate of anoxic respiration, by varying these one by one. We also conducted two transition tests to study the model response to changing WTD and anoxic respiration rate. In those, the model was first equilibrated with one set of driver values and after that the WTD or anoxic respiration was alternated. The different input combinations, details of the tests and their names are summarized in Tables 2 and 3.

The tests are named so that the first letter (T for temperature, W for WTD, L for LAI and R for respiration) tells which input varied and the rest shows the values of the constant input variables, with the simplification that W03 stands for WTD of -0.3 m. The transition test names just show the changing variables; Wtr stands for WTD transition and Rtr for respiration transition. The input range for LAI was based on, e.g., Slevin et al. (2015) and range of anoxic respiration on, e.g., Scanlon and Moore (2000) and Szafranek-Nakonieczna and Stepniewska (2014). In these tests we used a value of 0.5 for the parameter  $f_m$  (Table 1), the fraction of anaerobic respiration converted to  $\text{CH}_4$ , which was different from the value used for Siikaneva (0.25; see



Sect. 3.2.2). However, this parameter practically only controls the output CH<sub>4</sub> emission levels, and its effects on the model dynamics are minor.

In these tests, the anoxic respiration rate was always allocated only to the inundated peat layers. Consequently, when the WTD varied, also the number of layers into which the anoxic respiration was allocated varied, although the total respiration rate of the peat column remained constant. Temperature was always constant throughout the soil profile in these experiments, unlike in the simulations of the Siikaneva site.

### 3.2.2 Testing model sensitivity to the description of the peat column

We ran the model with a seven-year input data series from the Siikaneva fen (see Sect. 3.3 and App. B) and tested how sensitive the results are to peat depth and peat layer thicknesses. We used the same input anoxic respiration, WTD and LAI for all the model runs. The only factor that changed slightly between the different set-ups was the soil temperature since the temperature profile always followed the layering. The model spin-up was conducted by running the model through the entire seven-year time series of input data until the peat CH<sub>4</sub> concentrations stabilized. The spin-up time depended on the peat thickness, being 10...50 cycles.

15

We tested four peat depths, 1 m, 2 m, 3 m and 5 m using 0.2 m layer thickness in every case. In addition, we tested two evenly spaced layerings, 0.1 and 0.2 m, as well as one logarithmic layer structure, in a 2 m deep peat column. The logarithmic structure was based on the one used in the land surface model JSBACH (Ekici et al., 2014) and the layer thicknesses from top to bottom were 0.06, 0.13, 0.26, 0.52 and 1.03 m.

### 20 3.2.3 Intercomparison of HIMMELI and measured CH<sub>4</sub> fluxes in the Siikaneva site

We compared the CH<sub>4</sub> fluxes simulated when testing the model sensitivity to peat column description with CH<sub>4</sub> fluxes observed at Siikaneva. The purpose of this intercomparison was a general evaluation of how well HIMMELI is able to simulate the observations and what is its significance compared to using (simulated) anoxic respiration rate directly as the basis of CH<sub>4</sub> emission estimations. When comparing model and measurements, the dataset consisted only of those days from which the measured CH<sub>4</sub> flux was available.

### 3.3 Siikaneva site and measurements

The eddy covariance flux measurement site is located in Siikaneva in Ruovesi, Southern Finland (61°49' N, 24°11' E, 162 m a.s.l.) (Rinne et al., 2007). The site is a boreal oligotrophic fen where the vegetation is dominated by sedges (*C. rostrata*, *C. limosa*, *E. vaginatum*), Rannoch-rush (*Scheuchzeria palustris*) and peat mosses (*Sphagnum balticum*, *S. majus*, *S. papillosum*). Peat depth at the measurement footprint is 2...4 m. Annual mean temperature in 1971...2000 at a nearby weather station was 3.3° C and precipitation 713 mm (Drebs et al., 2002).

30



We drove the model with daily averages of WTD, peat temperature profile, LAI and anoxic respiration rate, and compared the results with daily medians of CH<sub>4</sub> flux data from years 2005...2011. Simulation of LAI and anoxic respiration are described in Appendix B. Peat temperature has been monitored in Siikaneva at five depths: -5 cm, -10 cm, -20 cm, -35 cm and -50 cm.

5 We created the temperature profile by interpolating linearly between the measurements. To obtain temperatures below the -50 cm depth we assumed that the temperature at -3 meters depth is constant at +7°C that was the mean temperature of all the years at -50 cm depth according to the measurements. Gaps in the measurement data were filled by linear interpolation. Soil temperature data from levels -10 and -40 cm was missing over a longer period so this gap was filled by linear interpolation between the adjacent measurement depths. The main component of the input anoxic respiration was derived from simulated

10 NPP. The NPP model was driven with the WTD, photosynthetically active radiation (PAR) and air temperature (T<sub>air</sub>). Long gaps in PAR and T<sub>air</sub> data were filled by using corresponding data from a nearby measurement station SMEAR II (Hari and Kulmala, 2005).

The measurement setup for CH<sub>4</sub> fluxes consisted of an acoustic anemometer and a fast response CH<sub>4</sub> analyzer. The acoustic

15 anemometer was Metek USA-1 during the whole measurement period, while there were changes in the methane analyzers. The CH<sub>4</sub> analyzers used were Campbell TGA-100 (2005...2007 and 04/2010...08/2010), Los Gatos RMT-200 (2008...2011) and Picarro G1301-f (04/2010...10/2011). For CO<sub>2</sub> and water vapor fluxes a closed path infrared absorption gas analyzer LiCor 7000 was used. The sonic anemometer and the intake for the CH<sub>4</sub> analyzer were at 2.75 m from peat surface. The sample air taken to the TGA-100 was dried using Nafion drier. For RMT-200 and G1301-f sample air was not dried. The measurement

20 setup for 2005...2007 has been described in detail by Aurela et al. (2007) and Rinne et al. (2007).

The flux data were post-processed using EddyUH software (Mammarella et al., 2016). The fluxes were calculated using block-averaging and sector-wise planar fitting. High frequency losses were corrected by empirically determined transfer functions (Mammarella et al., 2009). For 2008...2011, the dilution effect by water vapor were corrected with Webb-Leuning-Pearman

25 method (Webb et al., 1980), whereas for 2005...2007 this correction was not needed due to the usage of a drier in the sampling line.

## 4 Results and discussion

### 4.1 Model sensitivity to input data

Via the tests, we wanted to verify that the model dynamics are robust, and to find out how sensitive the output CH<sub>4</sub> fluxes are

30 to the input data. Table 4. summarizes the sensitivity results. In the following, we discuss the results, focusing on the most important aspects and primarily on CH<sub>4</sub>. It is worth noting that these are results from mechanistic sensitivity tests of HIMMELI and not predictions about responses of CH<sub>4</sub> emissions to environmental factors in peatland ecosystems. For example, the total



input anoxic respiration rate here was independent of WTD. WTD only governed the number of peat layers into which this input was distributed.

According to the model, the steady-state dissolved CH<sub>4</sub> concentrations increase when moving deeper in the peat column (Fig. 2). This results from the increasing hydrostatic pressure that controls the threshold concentration (pressure) above which gases are released as ebullition. As the solubility of CO<sub>2</sub> is higher than that of CH<sub>4</sub>, the saturated CO<sub>2</sub> concentrations were higher than CH<sub>4</sub> concentrations. In the example shown here, ebullition was driven by CO<sub>2</sub>. This can be seen in the concentration plots: CH<sub>4</sub> concentrations did not saturate at their highest values but into a value in which the sum of the partial pressures of N<sub>2</sub>, CO<sub>2</sub> and CH<sub>4</sub> was in balance with the combined atmospheric and hydrostatic pressures. LAI was 0 and thus the only transport route of O<sub>2</sub> into the soil was diffusion in water-filled peat pores, therefore, O<sub>2</sub> concentrations remained very low.

Contribution of different transport routes in the total CH<sub>4</sub> flux varied according to model input. Naturally, when LAI was 0, no CH<sub>4</sub> was emitted via plants. Furthermore, because ebullition occurring when WTD was below the peat surface was transferred to the lowest air-filled peat layer and the gases continued via diffusion in dry peat or plant roots after that (see Sect. 3.1.7), the direct ebullition fluxes to the atmosphere were zero when WTD was below the peat surface. Increasing LAI increased the relative contribution of plant transport in the total CH<sub>4</sub> emission in tests L\_W0\_T10\_R1 and L\_W03\_T10\_R1 (Fig 3a; Table 4). Generally, the proportion of plant transport in the total CH<sub>4</sub> emissions correlated negatively with the total emission rate, which can be seen in particular in the test R\_W0\_L1\_T10 where LAI was constant 1 and input respiration varied (Fig. 3b). The underlying mechanism here was that high input respiration, i.e. high CH<sub>4</sub> and CO<sub>2</sub> production, enhanced ebullition (or ebullition followed by transport via diffusion in soil layers above the WTD in cases with WTD < 0) – as could be expected.

Anoxic respiration rate and the corresponding potential methane production rate (PMP) (tests starting with R\_) governed the outputted CH<sub>4</sub> emissions. The total emissions depended strongly on the PMP and were only modestly modified by LAI and WTD. The dependency was linear with R<sup>2</sup> of 1.0 in the cases that LAI was zero and greater than 0.99 in the cases with LAI of 1 m<sup>2</sup> m<sup>-2</sup> (Fig. 4). The percentage of PMP released as CH<sub>4</sub> emission varied between 21% and (almost) 100%, the smallest percentages occurring with the lowest anoxic respiration rates. Generally, the lowest values were obtained from the test R\_W0\_L1\_T10 because this combination allowed the highest inhibiting effect by O<sub>2</sub> (the underlying mechanism is discussed below). The highest emissions occurred when both WTD and LAI were zero in test R\_W0\_L0\_T10. The strong dependency between anoxic respiration and CH<sub>4</sub> emission was also demonstrated in the transition test (Fig. 5). The increase/decrease in input respiration affected directly the output CH<sub>4</sub> emission rate.

In the tests in which the input respiration was constant and we analyzed the sensitivity of CH<sub>4</sub> fluxes to LAI, WTD and temperature, the final total steady-state CH<sub>4</sub> emission rates varied from 16% to almost 100% of PMP. All the test results



combined (Fig. 6), the most important governing factor seemed to be LAI; the high emissions required LAI being zero because that minimized the O<sub>2</sub> transport into the soil. Secondly, WTD controlled the fluxes. The highest emissions occurred when, in addition to zero LAI, WTD was zero or above the peat surface. Effect of temperature was the least important of the input factors, unlike probably in models that describe the total carbon cycle where the rate of anoxic respiration depends on temperature. However, also with HIMMELI the largest CH<sub>4</sub> emissions occurred in the tests with high temperatures.

One interesting result was that the CH<sub>4</sub> emissions decreased with decreasing WTD in test W\_L0\_T10\_R1 in which plant transport played no role (Fig. 7a). This was controlled by the oxidation rate that depends on the thickness of the dry oxic peat layer. However, when plant transport was included in W\_L1\_T10\_R1, the highest emissions occurred with the deepest WTD (Fig. 7b) because then the root mass available for transporting O<sub>2</sub> into the CH<sub>4</sub>-producing peat layers was at its lowest. The same trends were obvious in the transition tests with changing WTD (Wtr\_L1 and Wtr\_L0; Fig 8), dropping WTD caused increasing emissions when LAI was 1 but decreased them when LAI was 0.

The main conclusion that can be deduced from the results reviewed above is that O<sub>2</sub> concentration was an important player in the simulations. It affected both the inhibition of CH<sub>4</sub> production and oxidation of CH<sub>4</sub> to CO<sub>2</sub> (Equations 6 and 8). In the tests with constant input respiration (tests ending with \_R1), the actualized CH<sub>4</sub> production rate varied from 37% to (very close to) 100% of the PMP, and the highest inhibition of CH<sub>4</sub> production (i.e., lowest CH<sub>4</sub> production) occurred with high LAI that allowed high O<sub>2</sub> plant transport into the soil. The same pattern was obvious in the tests on varying input respiration (R\_). When LAI was zero, the CH<sub>4</sub> production was more or less equal to the PMP. When LAI was 1 and WTD was -0.3 m, the production was 93%...98% of the PMP. When LAI was 1 and WTD was 0, i.e., all the roots were inundated, the production was at its lowest and varied between 53% and 74% of PMP. This indicates that the more O<sub>2</sub> was transported to those soil layers that produced CH<sub>4</sub>, the less CH<sub>4</sub> was produced and consequently emitted. Whether the same production was distributed either in the entire 2 m peat column or only e.g. in the bottom 1.7 m, was significant since in the latter case, there was less O<sub>2</sub> transported as a whole to the CH<sub>4</sub>-producing soil layers, because the greatest root mass is allocated into the topmost peat layers.

The impact of temperature on the output fluxes was also transmitted via O<sub>2</sub> availability. A one-degree increase in peat temperature increased the total methane emissions on average by 0.10 nmol m<sup>-2</sup> s<sup>-1</sup> (0.02%) without gas-transporting vegetation (T\_W0\_L0\_R1) and 7.2 nmol m<sup>-2</sup> s<sup>-1</sup> (1.4%) with vegetation (T\_W0\_L1\_R1). The dependencies were linear with R<sup>2</sup> of 0.98 and 0.99, respectively. The main reason for this was that in cold temperatures, the solubility of gases, and thus the concentrations of dissolved O<sub>2</sub> in water were higher. Therefore, the CH<sub>4</sub> oxidation and inhibition of CH<sub>4</sub> production were highest in low temperatures although the rates of these reactions were at their lowest (Eq. 9).

The tests thus revealed that O<sub>2</sub> transport and other O<sub>2</sub>-related processes also deserve attention in CH<sub>4</sub> modelling, when O<sub>2</sub> concentrations are simulated. It is known that the strictly anoxic methanogens are inhibited by O<sub>2</sub> (Celis-García et al., 2004)



and so it is important to have a proper description of the inhibition process in the CH<sub>4</sub> models. O<sub>2</sub> transport of aerenchymatous plants has been measured in laboratory conditions (Moog and Brüggemann, 1998) and in the field (Mainiero and Kazda, 2004) but there seem to be no studies in which the simulated plant transport of O<sub>2</sub>, its dependency on model inputs like LAI or even the dissolved O<sub>2</sub> concentrations have been compared with measurements. Measuring O<sub>2</sub> fluxes with traditional chambers is  
5 challenging because detecting small changes in the high atmospheric O<sub>2</sub> concentration (21%) is difficult (Brix and Sorrell, 2013). Consequently, observational O<sub>2</sub> data for validating the O<sub>2</sub> side of CH<sub>4</sub> models is largely lacking.

As mentioned above, effects of the input factors on CH<sub>4</sub> emissions may be different when taking the whole peatland carbon cycle into consideration. For example, in test L\_W0\_T10\_R1 high LAI meant high CH<sub>4</sub> plant transport capacity that intuitively  
10 could mean high CH<sub>4</sub> emissions. However, here the impact of increased plant transport of O<sub>2</sub> into the soil was so strong that as a result, the total CH<sub>4</sub> emissions were lower with high LAI (Fig. 9). Root exudates of gas-transporting plants have been suggested to be a significant source of CH<sub>4</sub> substrates (Whiting and Chanton, 1993), and unlike in these sensitivity tests, a greater LAI would probably also mean higher CH<sub>4</sub> substrate input in nature. We tested this by setting the input respiration to depend linearly on LAI, assuming zero respiration when LAI=0. In this case, the total CH<sub>4</sub> emissions depended on the input  
15 respiration and increased with increasing LAI, as could be expected to happen when HIMMELI is connected to a full peatland carbon model.

Direct comparison of our results and sensitivity studies done on other peatland CH<sub>4</sub> emission models is not worthwhile because the other studies have analyzed the response of the total peatland carbon model. Some observations can, however, be made. In  
20 several studies the parameters affecting the CH<sub>4</sub> production rate have been found important (Wania et al., 2010; Berrittella and van Huissteden, 2011), which corresponds to our result that the input anoxic respiration rate affects the output significantly. Wania et al. (2010) tested the effect of tiller porosity on the CH<sub>4</sub> emissions and found that at four out of five of their sites, greater porosity increased the total CH<sub>4</sub> flux because of enhanced plant transport of CH<sub>4</sub>, despite the fact that also O<sub>2</sub> transport increased. However, in their model, O<sub>2</sub> did not affect the CH<sub>4</sub> production rate. In our tests, PMP was not dependent on  
25 temperature and hence the total effect of temperature was mediated via gas solubilities and rates of oxidation and inhibition. In a complete peatland model, also CH<sub>4</sub> production will depend on temperature and as the temperature sensitivity of CH<sub>4</sub> production is known to be high (Segers, 1998), probably that would outweigh the other temperature dependencies (Riley et al., 2011). Tang et al. (2010) studied the response of their models to changes in WTD and found that increasing the WTD retarded the CH<sub>4</sub> emissions probably because the diffusivity in water is lower than in the air. Whether the increasing WTD  
30 affected the total CH<sub>4</sub> production is not discussed in their study.

#### 4.2 Model sensitivity to the description of the peat column

The sensitivity tests with different soil layerings and peat thicknesses conducted using the input data set from Siikaneva site showed that the set-up of the peat column does not have any significant effect on the output. The mean total CH<sub>4</sub> flux was



- between 13 and 14  $\text{nmol m}^{-2} \text{s}^{-1}$  for all the set-ups. There were no striking differences in the simulated time series (Fig. 10) and so they all followed the measured  $\text{CH}_4$  fluxes similarly (Fig. 11a). The same applied to plant transport of  $\text{CH}_4$ ; the mean plant-transported flux was approximately 11  $\text{nmol m}^{-2} \text{s}^{-1}$  in all the cases. Direct ebullition to the atmosphere occurred only a few times during this seven-year simulation and so it was not a significant contribution to the total  $\text{CH}_4$  emissions (thus not shown).
- 5 The maximum peak direct ebullition to the atmosphere (daily average) fell between 1...15  $\text{nmol m}^{-2} \text{s}^{-1}$  in all the cases. The remains of the total flux, the mean being approximately 3  $\text{nmol m}^{-2} \text{s}^{-1}$  in each case, was transported by diffusion in the peat. This diffusion flux contained ebullited  $\text{CH}_4$  that originated from the water-filled peat layers when the WTD was below the peat surface, which was mostly the case.
- 10 This sensitivity test indicated that when simulating  $\text{CH}_4$  fluxes with HIMMELI, it is not worthwhile to describe a deep peat column with dense layering because it does not significantly improve the accuracy of the simulation compared with a faster set-up, such as a logarithmic layer structure that is often used in land surface models. The logarithmic layering gave – within the experimental accuracy – the same result as the 10 cm layers, when the input data was the same. The emission peaks of all the different set-ups coincided in 2010, despite the fact that the peat thicknesses differed. The underlying mechanism here was
- 15 that concentrations in pore water at certain depths always saturated at approximately similar levels and thus the sinking WTD triggered ebullition from the water-filled peat layers similarly in all the cases. The ebullited  $\text{CH}_4$  is seen as a peak in the diffusion flux. This may, however, depend on the WTD range used.

#### 4.3 Intercomparison of modelled and measured $\text{CH}_4$ fluxes

- Figure 11a shows the daily observed  $\text{CH}_4$  fluxes and the  $\text{CH}_4$  fluxes simulated using the logarithmic layer structure in a 2 m
- 20 deep peat column. The model followed the measurements reasonably but it underestimated the observed  $\text{CH}_4$  emissions on average by approximately 20%. The main reason for this discrepancy was that the anoxic respiration rate calculation (App. B) deviated from that of Susiluoto et al. (2017) and we did not optimize the parameters of HIMMELI specifically for the set-up of this study but used their parameter values as such. Simulation-based input data may also have caused the divergence between the model and measurements in the autumns when generally the modelled  $\text{CH}_4$  emissions seemed to decline too early.
- 25 Simulated NPP (that formed the main part of the anoxic respiration) or the LAI curve may have been biased or the way how the anoxic respiration depended on NPP may have been too straightforward. It now depended directly on the daily NPP and produced  $\text{CH}_4$  and  $\text{CO}_2$  immediately, there were no pools of potential  $\text{CH}_4$  substrates. In reality, as well as in soil carbon models with which HIMMELI could be combined, there is some lag in the process of carbon fixation turning into root exudates and further to  $\text{CH}_4$ .

30

Correlation between model and measurement (Fig. 11b) was relatively good and linear with low emissions but the scatter increased with emissions above 0.05  $\mu\text{mol m}^{-2} \text{s}^{-1}$ . The high simulated emissions were largely driven with ebullition – that in



most cases was emitted as diffusion of ebullited CH<sub>4</sub> from the air-filled peat layer – in summertime. The model was a slightly better predictor for the measured CH<sub>4</sub> emissions than the anoxic respiration as such (Fig. 11c), with  $R^2$  0.65 vs. 0.60. Hence, considering the anoxic respiration simulation combined with HIMMELI as one unified CH<sub>4</sub> model, HIMMELI improved the fit compared with the anoxic respiration part alone. This shows that HIMMELI is capable of simulating realistic CH<sub>4</sub> fluxes.

5

In the data set shown in the correlation plots, which was limited to those days from which the measured CH<sub>4</sub> fluxes were available, the  $R^2$  between input anoxic respiration and modelled CH<sub>4</sub> emissions was 0.69. In the complete simulated time series, this  $R^2$  was 0.79 and when correlating the CH<sub>4</sub> emissions with anoxic respiration of the previous day,  $R^2$  still slightly increased, up to 0.80. In the complete time series, the simulated CH<sub>4</sub> emissions were on average 14% of the input anoxic respiration or 10 56% of PMP. These results support the findings from the sensitivity tests (Section 4.1) that anoxic respiration rate and the corresponding PMP do govern the output CH<sub>4</sub> emissions, but indicate also that oxidation and inhibition played a role in the site simulation of Siikaneva.

Anoxic respiration alone thus seems a good basis to estimate CH<sub>4</sub> emissions but a complete model of CH<sub>4</sub> processes is 15 necessary, also in situations when the focus is not on studying concentration profiles or the processes in detail. Simple parameterizations have been tested against process-based CH<sub>4</sub> models. For example, Van Huissteden et al. (2009) compared the peatland model PEATLAND-VU that utilizes the Walter-Heimann CH<sub>4</sub> scheme, with an emission factor that was based on averages of measurement data on six arctic and temperate wetlands. They found that the model produced a significantly better estimate only on 50% of the sites; on the others, the simple emission factor did better or almost equally well. They 20 concluded, however, that process models are needed for large-scale modelling. Berrittella and van Huissteden (2009) compared PEATLAND-VU to a fixed fraction of NPP as the estimate of CH<sub>4</sub> emissions when simulating northern wetlands in glacial climates. In this case, they naturally did not have real-time observational flux data to compare their results with, but they concluded that the two approaches gave *different* results, for instance, the simplistic NPP model produced smaller differences between glacial climates than PEATLAND-VU. A CH<sub>4</sub> model like HIMMELI is a significant addition to peatland carbon 25 models, in order to be able to take into account more factors affecting CH<sub>4</sub> emissions.

## 5 Conclusions

The new model for simulating CH<sub>4</sub> build-up and emissions in peatlands, HIMMELI, is a robust tool to be used as the CH<sub>4</sub> emission model in different peatland carbon models. It runs well with different peat column set-ups and within a wide range of inputs. The simulated CH<sub>4</sub> emissions are not sensitive to the description of the peat column in case it does not affect the 30 input variables. HIMMELI was able to simulate CH<sub>4</sub> fluxes observed at the Siikaneva peatland measurement site in southern Finland when run with measured and simulated input from the site.



Sensitivity tests conducted on HIMMELI revealed mechanisms controlling the simulated CH<sub>4</sub> emissions that may remain hidden when testing the sensitivity of a full peatland carbon cycle model. Simulated CH<sub>4</sub> fluxes largely depended on the input anoxic respiration rate and the corresponding CH<sub>4</sub> production rate. This shows that in addition to correct descriptions of CH<sub>4</sub> and O<sub>2</sub> transport and oxidation processes, it is essential that the underlying CH<sub>4</sub> substrate production rates are realistic, in order to produce realistic CH<sub>4</sub> emission estimates for different purposes. Other input variables, in particular LAI and WTD, also had an impact on the CH<sub>4</sub> emissions in the steady-state tests. With constant input anoxic respiration (which means constant potential CH<sub>4</sub> production rate), the total CH<sub>4</sub> emission varied from 16 % to almost 100 % of the potential CH<sub>4</sub> production, depending on the combination of LAI and WTD. The results indicated that the main factor governing this was the availability of O<sub>2</sub> in the peat since its concentration affected the inhibition of CH<sub>4</sub> production as well as rates of CH<sub>4</sub> oxidation to CO<sub>2</sub>.

## 6 Code and data availability

The FORTRAN codes of the HIMMELI model are available as a supplement of this article. The data used in these analyses are available upon request.

## Appendix A

The solubilities of gases are computed following Sander (2015). The temperature (T) dependence of Henry's law constants for the three simulated compounds CH<sub>4</sub>, CO<sub>2</sub> and O<sub>2</sub> ( $H_X$ ; M atm<sup>-1</sup>) thus are (Eq. A1-A3):

$$H_{CH_4}(T) = 1.3 \times 10^{-3} \exp \left[ 1700 \left( \frac{1}{T} - \frac{1}{T^{\theta}} \right) \right] \quad (A1)$$

$$H_{O_2}(T) = 1.3 \times 10^{-3} \exp \left[ 1500 \left( \frac{1}{T} - \frac{1}{T^{\theta}} \right) \right] \quad (A2)$$

$$H_{CO_2}(T) = 3.4 \times 10^{-2} \exp \left[ 2400 \left( \frac{1}{T} - \frac{1}{T^{\theta}} \right) \right], \quad (A3)$$

where  $T^{\theta}$  is the reference temperature, 298 K. Temperature dependent diffusivities of the three compounds in water ( $D_{X,w}$ ; m<sup>2</sup> s<sup>-1</sup>) and in air ( $D_{X,a}$ ; m<sup>2</sup> s<sup>-1</sup>) are calculated following Tang et al. (2010) (Eq. A4-A9). The reference temperature  $T^{\theta b}$  used in Equations A7-A9 is 273.15 K.

$$D_{CH_4,w}(T) = 1.5 \times 10^{-9} \frac{T}{T^{\theta}} \quad (A4)$$

$$D_{O_2,w}(T) = 2.4 \times 10^{-9} \frac{T}{T^{\theta}} \quad (A5)$$

$$D_{CO_2,w}(T) = 1.81 \times 10^{-6} \exp \left( \frac{-2032.6}{T} \right) \quad (A6)$$



$$D_{CH_4,a}(T) = 1.9 \times 10^{-5} \left( \frac{T}{T_{\theta b}} \right)^{1.82} \quad (A7)$$

$$D_{O_2,a}(T) = 1.8 \times 10^{-5} \left( \frac{T}{T_{\theta b}} \right)^{1.82} \quad (A8)$$

$$D_{CO_2,a}(T) = 1.47 \times 10^{-5} \left( \frac{T}{T_{\theta b}} \right)^{1.792} \quad (A9)$$

## Appendix B

- 5 LAI is not continuously monitored at Siikaneva, therefore, we utilized the method introduced by Wilson et al. (2007) to obtain LAI input data for the Siikaneva model runs. We simulated the LAI with a lognormal function (Wilson et al., 2007) (Eq. B1):

$$LAI(j) = LAI_{max} \times e^{\left( -0.5 \left( \frac{\ln\left(\frac{j}{j_{max}}\right)}{s} \right)^2 \right)} \quad (B1)$$

- 10 where  $LAI_{max}$  is the peak LAI of the growing season,  $j$  is the Julian date,  $j_{max}$  is the Julian date when the LAI peaks, and  $s$  denotes the shape of the curve. Values for the parameters  $j_{max}$  and  $s$  (Table B1) were derived from Wilson et al. (2007) by averaging the values reported for the species abundant at Siikaneva. The growing season peak LAI in the eddy covariance footprint area at Siikaneva was approximately  $0.4 \text{ m}^2 \text{ m}^{-2}$  (Riutta et al., 2007). We also chose to add a constant wintertime LAI in the model since it is known that a significant green sedge biomass, approximately 15% of the maximum, may overwinter  
15 (Bernard and Hankinson, 1979; Saarinen, 1998). The maximum being  $0.4 \text{ m}^2 \text{ m}^{-2}$ , the overwintering LAI would thus be up to  $0.05 \text{ m}^2 \text{ m}^{-2}$ . We used the same LAI for all the years.

- The input anoxic respiration was estimated following closely the parallel study Susiluoto et al. (2017) in which the HIMMELI parameters were optimized for Siikaneva. Susiluoto et al. (2017) simulated production of  $CH_4$  substrates as temperature-  
20 dependent anoxic peat decomposition  $V_{pR}$  ( $\text{mol m}^{-2} \text{ s}^{-1}$ ) and decomposition of root exudates in the inundated peat layers. This was computed with a simple respiration model combined with HIMMELI. Since in the present study the focus was on testing the HIMMELI model as such, we did not involve the complete respiration model here but produced input for HIMMELI using the same components as Susiluoto et al. (2017) in a simplified form. The input respiration in our study was simply the sum of anoxic peat decomposition rate and estimated root exudate production  $V_{exu}$  ( $\text{mol m}^{-2} \text{ s}^{-1}$ ) in the inundated peat layers, we did  
25 not simulate the actual decomposition of the root exudate pool. The soil profile for which the respiration was computed was 2 m of peat with 0.1 m layers.



$V_{exu}$  was estimated by taking a fixed fraction  $f_{exu}$  of the net primary productivity (NPP) of vascular vegetation, i.e., simulated net photosynthesis rate  $P_n$  ( $\text{mol m}^{-2} \text{s}^{-1}$ ) of vascular plants.  $f_{exu}$  (Table B1) was obtained from Susiluoto et al. (2017) and the NPP was calculated by running models of gross photosynthesis ( $P_g$ ) and autotrophic respiration ( $R$ ) for Siikaneva. We used the  $P_g$  model for a sedge and dwarf shrub canopy by Riutta et al. (2007) (Eq. B2):

$$5 \quad P_g = P_{max} \frac{I}{h+I} [1 - e^{-a \times LAI}] \times e^{-0.5 \left( \frac{T_{air} - T_{opt}}{T_{tol}} \right)^2} \times e^{-0.5 \left( \frac{d_W - d_{W,opt}}{d_{W,tol}} \right)^2} \quad (\text{B2})$$

where  $P_g$  is the  $\text{CO}_2$  uptake rate of the canopy ( $\text{mol CO}_2 \text{s}^{-1} \text{m}^{-2}$  ground surface area),  $P_{max}$  is the maximum potential  $\text{CO}_2$  uptake rate ( $\text{mol CO}_2 \text{s}^{-1} \text{m}^{-2}$  ground surface area),  $I$  ( $\mu\text{mol m}^{-2} \text{s}^{-1}$ ) is PAR,  $h$  ( $\mu\text{mol m}^{-2} \text{s}^{-1}$ ) is PAR at which half of maximum photosynthesis is reached,  $a$  is the initial slope of saturating leaf-area response function, LAI is leaf area index (Eq. B1),  $T_{air}$  ( $^\circ\text{C}$ ) is air temperature,  $T_{opt}$  ( $^\circ\text{C}$ ) is the optimal air temperature for photosynthesis,  $T_{tol}$  ( $^\circ\text{C}$ ) is temperature tolerance,  $d_W$  (cm) is WTD,  $d_{W,opt}$  (cm) is the optimal WTD for photosynthesis, and  $d_{W,tol}$  (cm) is WTD tolerance. The parameter values are listed in Table B1.  $R$  ( $\text{mol CO}_2 \text{s}^{-1} \text{m}^{-2}$ ) was simulated with a model parameterized for sedges only (Raivonen et al., 2015) (Eq. B3):

$$10 \quad R = R_{ref} \times LAI \times e^{b \left( \frac{1}{T_{ref} - T_0} - \frac{1}{T_{air} - T_0} \right)} \times e^{-0.5 \left( \frac{d_W - d_{W,opt}}{d_{W,tol}} \right)^2}, \quad (\text{B3})$$

where  $R$  is the  $\text{CO}_2$  release rate of the canopy,  $R_{ref}$  ( $\text{mol CO}_2 \text{s}^{-1} \text{m}^{-2}$  leaf area) is the  $\text{CO}_2$  release rate per unit of leaf area under reference conditions,  $b$  (K) is an exponential parameter depicting the temperature sensitivity of respiration,  $T_{ref}$  (K) is the reference temperature, and  $T_0$  (K) is the temperature at which respiration reaches zero (Table B1).

The daily averages of net photosynthesis  $P_n$  ( $\text{mol CO}_2 \text{s}^{-1} \text{m}^{-2}$ ) were calculated as the difference between  $P_g$  and  $R$ . Photosynthetically active seasons were determined by searching for dates of snowmelt in spring or arrival of snow cover in autumn from the reflected PAR data or, in some cases, using air temperature (permanently  $> 5^\circ\text{C}$ ) as the criterion. No direct measurements of  $P_n$  or vascular NPP exist for validation but the simulated  $P_n$  of year 2005 was compared with an NPP estimate derived from eddy covariance  $\text{CO}_2$  fluxes measured that year on Siikaneva. Briefly, the estimated contributions of *Sphagnum* mosses (30%; Riutta et al., 2007) and autotrophic respiration (50%; Gifford, 1994) were subtracted from the eddy-covariance based gross primary productivity (GPP) (Aurela et al., 2007; data obtained via personal communication), and the remains were taken as an estimate of the NPP of vascular vegetation. The two NPP estimates were well correlated (with  $R^2$  of 0.9) but the eddy-covariance based NPP was on average 1.56-fold compared with the simulated  $P_n$ . Since the latter also was lowish compared with what has been reported for similar peatlands, the final estimate of NPP for years 2005...2011 was produced by scaling the simulated  $P_n$  upwards by 1.56.

The anoxic peat respiration was computed for the peat layers below WTD using the  $Q_{10}$  model for catotelm decomposition presented in Schuldt et al. (2013) (Eq. B4):



$$V_{pR} = \sum_{z_{min}}^{WTD} Q_{10} \frac{T(z)-T_{ref,pR}}{10} \frac{1}{\tau_c} \rho_C dz. \quad (B4)$$

Here  $Q_{10}$  is the base for temperature dependence of respiration,  $T_{ref,pR}$  is reference temperature for peat respiration (K),  $\tau_{cato}$  is turnover time of the catotelm carbon pool (s) and  $\rho_C$  (mol (C) m<sup>-3</sup>) is the density of the carbon pool. The parameter set optimized by Susiluoto et al. (2017) included  $Q_{10}$  and  $\tau_c$ , the other values were taken from Schuldt et al. (2013) (Table 1).

## 5 [Supplement link]

*Author contribution:* M. Raivonen participated in model development and designed and carried out the tests with contribution from L. Backman, J. Susiluoto, T. Aalto, T. Markkanen, J. Mäkelä and T. Vesala. S. Smolander and L. Backman developed the model. M. Tomasic, X. Li, M. Heimann, S. Sevanto, T. Kleinen and V. Brovkin contributed to the model development. J. Rinne, O. Peltola and M. Aurela provided observational data from the Siikaneva site. T. Larmola, S. Juutinen and E.-S. Tuittila provided knowledge and advice about peatland methane processes for model development. M. Raivonen prepared the manuscript with contributions from all co-authors.

## Competing interests

The authors declare that they have no conflict of interest.

## 15 Acknowledgements

We thank the Academy of Finland Center of Excellence (272041), Academy Professor projects (284701 and 282842), CARB-ARC (285630), ICOS Finland (281255), NCoE eSTICC (57001), EU-H2020 CRESCENDO (641816) and MONIMET (LIFE07 ENV/FIN/000133) and Maj and Tor Nessling Foundation (projects 2008336, 2009067 and 2010212) for support. Academy of Finland is also acknowledged by E.-S.T. (project 287039) and T.L. (121535, 286731 and 293365). T.K. acknowledges funding by the German ministry for research (BMBF) in projects CarboPerm and PalMod.

## References

Arah, J. R. M. and Stephen, K. D.: A model of the processes leading to methane emission from peatland – kinetics of CH<sub>4</sub> and O<sub>2</sub> removal and the role of plant roots, *Atm. Env.*, 32(19), 3257–3264, 1998.  
Aurela, M., Riutta, T., Laurila, T., Tuovinen, J.-P., Vesala, T., Tuittila, E.-S., Rinne, J., Haapanala, S., and Laine, J.: CO<sub>2</sub> exchange of a sedge fen in southern Finland – the impact of a drought period, *Tellus*, 59B, 826-837, 2007.



- Baird, A. J., Beckwith, C. W., and Waldron, S.: Ebullition of methane-containing gas bubbles from near-surface Sphagnum peat, *Geophys. Res. Lett.*, 31(21), doi: 10.1029/2004GL021157, 2004.
- Bergman, I., Lundberg P., and Nilsson, M.: Microbial carbon mineralization in an acid surface peat: effects of environmental factors in laboratory incubations, *Soil Biol. Biochem.*, 31, 1867-1877, 1999.
- 5 Bernard, J. M., and Hankinson, G.: Seasonal changes in standing crop, primary production, and nutrient levels in a *Carex rostrata* wetland, *Oikos*, 32, 328-336, 1979.
- Berrittella, C. and van Huissteden, J.: Uncertainties in modelling CH<sub>4</sub> emissions from northern wetlands in glacial climates: effect of hydrological model and CH<sub>4</sub> model structure, *Clim. Past*, 5, 361–373, 2009.
- Berrittella, C. and van Huissteden, J.: Uncertainties in modelling CH<sub>4</sub> emissions from northern wetlands in glacial climates: the role of vegetation parameters, *Clim. Past*, 7, 1075-1087, 2011.
- 10 Bird, R. B., Stewart, W. E. and Lightfoot, E. N.: *Transport Phenomena*, John Wiley and Sons, New York, USA, 1960.
- Bon, C. E., Reeve, A.S., Slater, L., and Comas, X.: Using hydrologic measurements to investigate free-phase gas ebullition in a Maine peatland, USA, *Hydrol. Earth Syst. Sci.*, 18, 953-965, 2014.
- Bridgham, S. D., Cadillo-Quiroz, H., Keller, J. K., and Zhuang, Q.: Methane emissions from wetlands: biogeochemical, microbial and modelling perspectives from local to global scales, *Glob. Change Biol.*, 9(5), 1325-1346. doi: 10.1111/gcb.12131, 2013.
- 15 Brix, H., Sorrell, B. K., and Schierup, H. H.: Gas fluxes achieved by in-situ convective flow in *Phragmites australis*, *Aquat. Bot.*, 54, 2-3, 151-163, 1996.
- Brix, H. and Sorrell, B. K.: Gas transport and exchange through wetland plant aerenchyma, in: *Methods in Biogeochemistry of Wetlands*, DeLaune, R. D., Reddy, K. R., Richardson, C. J., and Megonigal, J. P. (Eds.), SSSA Book Series no. 10, Soil Science Society of America, Madison, USA, 177-196, 2013.
- Budishchev, A., Mi, Y., van Huissteden, J., Beilelli-Marchesini, L., Schaeppman-Strub, G., Parmentier, F. J. W., Fratini, G., Gallagher, A., Maximov, T. C., and Dolman, A. J.: Evaluation of a plot-scale methane emission model using eddy covariance observations and footprint modelling, *Biogeosciences*, 11, 4651-4664, 2014.
- 25 Celis-García, M. L. B., Ramírez, F., Revah, S., Razo-Flores, E., and Monroy, O.: Sulphide and oxygen inhibition over the anaerobic digestion of organic matter: influence of microbial immobilization type. *Environ. Technol.*, 25(11), 1265-1275, 2004.
- Chanton, J. P. and Whiting, G. J.: Methane stable isotopic distributions as indicators of gas transport mechanisms in emergent aquatic plants. *Aquat. Bot.* 54, 227-236, 1993.
- 30 Ciais, P., Sabine, C., Bala, G., Bopp, L., Brovkin, V., Canadell, J., Chhabra, A., DeFries, R., Galloway, J., Heimann, M., Jones, C., Le Quéré, C., Myneni, R. B., Piao, S., and Thornton, P.: Carbon and Other Biogeochemical Cycles. In: *Climate Change 2013: The Physical Science Basis. Contribution of Working Group I to the Fifth Assessment Report of the Intergovernmental Panel on Climate Change* [Stocker, T.F., D. Qin, G.-K. Plattner, M. Tignor, S.K. Allen, J. Boschung, A.



- Nauels, Y. Xia, V. Bex and P.M. Midgley (Eds.]. Cambridge University Press, Cambridge, United Kingdom and New York, NY, USA, 2013.
- Collin, M. and Rasmuson, A.: A comparison of gas diffusivity models for unsaturated porous media, *Soil Sci. Soc. Am. J.*, 52, 1559-1565, 1988.
- 5 Colmer, T. D.: Long-distance transport of gases in plants: a perspective on internal aeration and radial oxygen loss from roots, *Plant Cell Environ.*, 26(1), 17-36, 2003.
- Comas, X., Slater, S., and Reeve, A.S.: Atmospheric pressure drives changes in the vertical distribution of biogenic free-phase gas in a northern peatland, *J. Geophys. Res.*, 116, G04014, doi:10.1029/2011JG001701, 2011.
- Coulthard, T. J, Baird, A. J., Ramirez, J., and Waddington, J. M.: Methane dynamics in peat: importance of shallow peats and a novel reduced-complexity approach for modeling ebullition, in: *Geophysical Monograph Series, Carbon Cycling in Northern Peatlands*, 184, 173, doi:10.1029/2008GM000811, 2009.
- 10 Cresto Aleina, F., Runkle, B. R. K., Kleinen, T., Kutzbach, L., Schneider, J., and Brovkin, V.: Modeling micro-topographic controls on boreal peatland hydrology and methane fluxes, *Biogeosciences*, 12, 5689-5704, 2015.
- Drebs, A., Nordlund, A., Karlsson, P., Helminen, J., and Rissanen, P.: Climatological statistics of Finland 1971-2000, Finnish Meteorological Institute, Helsinki, 99 ISBN 951-697-568-2, 2002.
- 15 Ekici, A., Beer, C., Hagemann, S., Boike, J., Langer, M., and Hauck, C.: Simulating high-latitude permafrost regions by the JSBACH terrestrial ecosystem model, *Geosci. Model Dev.*, 7, 631-647, doi:10.5194/gmd-7-631-2014, 2014.
- Estop-Aragónés, C., Klaus-Holger, K., and Blodau, C.: Controls on in situ oxygen and dissolved inorganic carbon dynamics in peats of a temperate fen, *J. Geophys. Res.*, 117, doi:10.1029/2011JG001888, 2012.
- 20 Fan, Z., Neff, J. C., Waldrop, M. P., Ballantyne, A. P., and Turetsky, M. R.: Transport of oxygen in soil pore-water systems: implications for modeling emissions of carbon dioxide and methane from peatlands, *Biogeochemistry*, 121(3), 455-470, 2014.
- Fritz, C., Pancotto, V. A., Elzenga, J. T. M., Visser, E. J. W., Grootjans, A. P., Pol, A., Iturraspe, R., Roelofs, J. G. M., and Smolders, A. J. P.: Zero methane emission bogs: extreme rhizosphere oxygenation by cushion plants in Patagonia, *New Phytol.*, 190, 398-408, 2011.
- 25 Gifford, R. M.: The global carbon cycle: a viewpoint on the missing sink, *Aust. J. Plant Physiol.*, 21, 1-15, 1994.
- Glaser, P. H., Chanton, J. P., Morin, P., Rosenberry, D. O., Siegel, D. I., Ruud, O., Chasar, L. I., and Reeve, A. S.: Surface deformations as indicators of deep ebullition fluxes in a large northern peatland, *Global Biogeochem. Cy.*, 18, GB1003, doi: 10.1029/2003GB002069, 2004.
- Grant, R. F. and Roulet, N.T.: Methane efflux from boreal wetlands: Theory and testing of the ecosystem model Ecosys with chamber and tower flux measurements, *Global Biogeochem. Cy.*, 16(4), 1054, doi:10.1029/2001GB001702, 2002.
- 30 Grant, R. F., Humphreys, E. R., and Lafleur, P. M.: Ecosystem CO<sub>2</sub> and CH<sub>4</sub> exchange in a mixed tundra and a fen within a hydrologically diverse arctic landscape: 1. Modeling versus measurements, *Biogeosciences*. Vol.120, Issue 7, 1366–1387, 2015.



- Green, S.M. and Baird, A. J.: A mesocosm study of the role of the sedge *Eriophorum angustifolium* in the efflux of methane—including that due to episodic ebullition—from peatlands, *Plant Soil*, 351, 207-218, 2012.
- Haario, H., Saksman, E., and Tamminen, J.: An adaptive Metropolis algorithm, *Bernoulli*, 7(2), 223-242, 2001.
- Hari, P. and Kulmala, M.: Station for Measuring Ecosystem-Atmosphere Relations (SMEAR II), *Boreal Environment*
- 5 *Research*, 10, 315–322, 2005.
- Hennenberg, A., Sorrell, B. K., and Brix H.: Internal methane transport through *Juncus effusus*: experimental manipulation of morphological barriers to test above- and below-ground diffusion limitation, *New Phytol.*, 196, 799-806, 2012.
- Iiyama, I. and Hasegawa, S.: Gas diffusion coefficient of undisturbed peat soils, *Soil Sci. Plant Nutr.*, 51(3), 431-435, 2005.
- Jackowicz-Korczyński, M., Christensen, T. R., Bäckstrand, K., Crill, P., Friborg, T., Mastepanov, M., and Ström, L.: Annual
- 10 cycle of methane emission from a subarctic peatland, *Biogeosciences*, 115, doi: 10.1029/2008JG000913, 2010.
- Juutinen, S., Alm, J., Larmola, T., Saarnio, S., Martikainen, P.J., and Silvola J.: Stand-specific diurnal dynamics of CH<sub>4</sub> fluxes in boreal lakes: Patterns and controls, *J. Geophys. Res.*, 109(D19313), doi:10.1029/2004JD004782, 2004.
- Kelker, D. and Chanton, J.: The effect of clipping on methane emissions from *Carex*, *Biogeochemistry*, 39:37, doi:10.1023/A:1005866403120, 1997.
- 15 Kellner, E., Baird, A. J., Oosterwoud, M., Harrison, K., and Waddington, J. M.: Effect of temperature and atmospheric pressure on methane (CH<sub>4</sub>) ebullition from near-surface peats, *Geophys. Res. Lett.*, 33, doi: 10.1029/2006GL027509, 2006.
- Khvorostyanov, D. V., Krinner, G., Ciais, P., Heimann, M., Zimov, S. A.: Vulnerability of permafrost carbon to global warming. Part I: model description and role of heat generated by organic matter decomposition, *Tellus B.* 60, 250–264, 2008.
- King, G. M.: Associations of methanotrophs with the roots and rhizomes of aquatic vegetation, *Appl. Environ. Microb.*, 60(9),
- 20 3220-3227, 1994.
- King, J. Y., Reeburgh, W. S., and Regli, S. K.: Methane emission and transport by arctic sedges in Alaska: Results of a vegetation removal experiment, *J. Geophys. Res.*, 103(D22), 29083-29092, 1998.
- Lai, D. Y. F.: Methane dynamics in northern peatlands: a review, *Pedosphere*, 19(4), 409-421, 2009.
- Macdonald, J. A., Fowler, D., Hargreaves, K. J., Skiba, U., Leith, I. D., and Murray, M. B.: Methane emission rates from a
- 25 northern wetland; response to temperature, water table and transport, *Atm. Env.*, 32(19), 3219-3227, 1998.
- Mainiero, R., Kazda, M.: Effects of *Carex rostrata* on soil oxygen in relation to soil moisture, *Plant Soil*, 270, 311-320, 2004.
- Mammarella, I., Launiainen, S., Gronholm, T., Keronen, P., Pumpanen, J., Rannik, Ü, and Vesala, T.: Relative humidity effect on the high-frequency attenuation of water vapor flux measured by a closed-path eddy covariance system, *J. Atmos. Ocean. Technol.*, 26 (9), 1856–1866, 2009.
- 30 Mammarella, I., Peltola, O., Nordbo, A., Järvi, L., and Rannik, Ü.: Quantifying the uncertainty of eddy covariance fluxes due to the use of different software packages and combinations of processing steps in two contrasting ecosystems, *Atmos. Meas. Tech.*, 9, 4915-4933, doi:10.5194/amt-9-4915-2016, 2016.
- Melton, J. R., Wania, R., Hodson, E. L., Poulter, B., Ringeval, B., Spahni, R., Bohn, T., Avis, C. A., Beerling, D. J., Chen, G., Eliseev, A. V., Denisov, S. N., Hopcroft, P. O., Lettenmaier, D. P., Riley, W. J., Singarayer, J. S., Subin, Z. Z. M., Tian, H.,



- Zürcher, S., Brovkin, V., van Bodegom, P. M., Kleinen, T., Yu, Z. C., and Kaplan, J. O.: Present state of global wetland extent and wetland methane modelling: conclusions from a model inter-comparison project (WETCHIMP), *Biogeosciences*, 10, 753-788, 2013.
- Mikkilä, C., Sundh, I., Svensson, B. H., and Nilsson, M.: Diurnal variation in methane emission in relation to the water table, soil temperature, climate and vegetation cover in a Swedish acid mire, *Biogeochemistry*, 28(2), 93-114, 1995.
- 5 Millington, R. J.: Gas diffusion in porous media, *Science*, 130, 100-102, 1959.
- Mitsch, W. J. and Gosselink, J. G.: *Wetlands*, John Wiley & Sons, New Jersey, USA. 582 p, 2007.
- Moog, P. R. and Brüggeman, W.: Flooding tolerance of *Carex* species. II. Root gas-exchange capacity, *Planta*, 207(2), 199-206, 1998.
- 10 Moore, T. R., DeYoung, A., Bubier, J. L., Humphreys, E. R., Lafleur, P. M., and Roulet, N. T.: A multi-year record of methane flux at the Mer Bleue Bog, southern Canada, *Ecosystems*, 14, 646-657, 2011.
- Morrissey, L. A., Zobel, D. B., and Livingston, G. P.: Significance of stomatal control on methane release from *Carex*-dominated wetlands, *Chemosphere*, 26(1-4), 339-355, 1993.
- Myhre, G., Shindell, D., Bréon, F.-M., Collins, W., Fuglestedt, J., Huang, J., Koch, D., Lamarque, J.-F., Lee, D., Mendoza, B., Nakajima, T., Robock, A., Stephens, G., Takemura, T., and Zhang, H.: Anthropogenic and Natural Radiative Forcing. In: *Climate Change 2013: The physical Science Basis. Contribution of Working Group I to the Fifth Assessment Report of the Intergovernmental Panel on Climate Change* [Stocker TF, Qin D, Plattner G-K, Tignor M, Allen SK, Boschung J, Nauels A, Xia Y, Bex V, Midgley PM (eds.)]. Cambridge University Press, Cambridge, United Kingdom and New York, NY, USA, 2013.
- 15 Nilsson, M. and Öquist, M.: Partitioning litter mass loss into carbon dioxide and methane in peatland ecosystems, *Geoph. Monog. Series*, 184, Carbon Cycling in Northern Peatlands, 131-144, 2009.
- Nouchi, I., Mariko, S., and Aoki, K.: Mechanism of methane transport from the rhizosphere to the atmosphere through rice plants, *Plant Physiol.*, 94, 59-66, 1990.
- Popp, T. J., Chanton, J. P., Whiting, G. J., and Grant, N.: Methane stable isotope distribution at a *Carex* dominated fen in North  
25 Central Alberta, *Global Biogeochem. Cy.*, 13(4), 1063-1077, 1999.
- Raivonen, M., Mäkiranta, P., Lohila, A., Juutinen, S., Vesala, T., and Tuittila, E.-S.: A simple CO<sub>2</sub> exchange model simulates the seasonal leaf area development of peatland sedges, *Ecol. Model.*, 314, 32-43, 2015.
- Reiche, M.: Effect of peat quality on microbial greenhouse gas formation in an acidic fen, *Biogeosciences*, 7, 187-198, 2010.
- Reid, M. C., Pal, D. S., and Jaffé, P. R.: Dissolved gas dynamics in wetland soils: root-mediated gas transfer kinetics  
30 determined via push-pull tracer tests, *Water Resour. Res.*, 51(9), 7343-7357, 2015.
- Riley, W. J., Subin, Z. M., Lawrence, D. M., Swenson, S. C., Torn, M. S., Meng, L., Mahowald, N. M., and Hess, P.: Barriers to predicting changes in global terrestrial methane fluxes: analyses using CLM4Me, a methane biogeochemistry model integrated in CESM, *Biogeosciences*, 8, 1925-1953, 2011.



- Ringeval, B., Friedlingstein, P., Koven, C., Ciais, P., de Noblet-Ducoudré, N., Decharme, B., and Cadule, P.: Climate-CH<sub>4</sub> feedback from wetlands and its interaction with the climate-CO<sub>2</sub> feedback, *Biogeosciences*, 8, 2137-2157, 2011.
- Rinne, J., Riutta, T., Pihlatie, M., Aurela, M., Haapanala, S., Tuovinen, J. P., Tuittila, E.-S., and Vesala, T.: Annual cycle of methane emission from a boreal fen measured by the eddy covariance technique, *Tellus B*, 59, 449–457, 2007.
- 5 Riutta, T., Laine, J., and Tuittila, E.-S.: Sensitivity of CO<sub>2</sub> exchange of fen ecosystem components to water level variation, *Ecosystems*, 10, 718-733, doi:10.1007/s10021-007-9046-7, 2007.
- Saarinen, T.: Biomass and production of two vascular plants in a boreal mesotrophic fen, *Can. J. Bot.*, 74, 934-938, 1996.
- Saarinen, T.: Demography of *Carex rostrata* in boreal mesotrophic fen: shoot dynamics and biomass development, *Ann. Bot. Fennici*, 35, 203-209, 1998.
- 10 Sander, R.: Compilation of Henry's law constants (version 4.0) for water as solvent, *Atmos. Chem. Phys.*, 15, 4399-4981, 2015.
- Scanlon, D. and Moore, T.: Carbon dioxide production from peatland soil profiles: the influence of temperature, oxic/anoxic conditions and substrate, *Soil Sci.*, 165(2), 153-160, 2000.
- Schimel, J. P.: Plant transport and methane production as controls on methane flux from arctic wet meadow tundra, *Biogeochemistry*, 28(3), 183-200, 1995.
- 15 Schuldt, R. J., Brovkin, V., Kleinen, T., and Winderlich, J.: Modelling Holocene carbon accumulation and methane emissions of boreal wetlands – an Earth system model approach, *Biogeosciences*, 10, 1659-1674, 2013.
- Segers, R.: Methane production and methane consumption: a review of processes underlying wetland methane fluxes, *Biogeochemistry*, 41, 23-51, 1998.
- 20 Shaver, G. R., and Cutler, J. C.: The vertical distribution of live vascular phytomass in cottongrass tussock tundra, *Arctic Alpine Res.*, 11(3), 335-342, 1979.
- Silins, U. and Rothwell, R. L.: Spatial patterns of aerobic limit depth and oxygen diffusion rate at two peatlands drained for forestry in Alberta, *Can. J. For. Res.*, 29, 53–61, 1999.
- Slevin, D., Tett, S. F. B. and Williams, M.: Multi-site evaluation of the JULES land surface model using global and local data, *Geosci. Model Dev.*, 8, 295-316, doi: 10-5194/gmd-8-295-2015, 2015.
- 25 Staunton, S.: Diffusion Processes, in: *Encyclopedia of Soil Science*, Chesworth W (Ed), Springer Netherlands, ISBN 978-1-4020-3994-2, 185-191, doi: 10.1007/978-1-4020-3995-9\_158, 2008.
- Stephen, K. D., Arah, J. R. M., Daulat, N., and Clymo, R. S.: Root-mediated gas transport in peat determined by Argon diffusion, *Soil Biol. Biochem.*, Vol 30(4), pp. 501-508, 1998.
- 30 Susiluoto, J., Raivonen, M., Mäkelä, J., Backman, L., Laine, M., Smolander, S., Aalto, T., and Vesala, T.: Enhancing the performance of a new methane model based on information from Bayesian model calibration. In preparation.
- Szafranek-Nakonieczna, A. and Stepniewska, Z.: Aerobic and anaerobic respiration in profiles of Polesie Lubelskie peatlands, *Int. Agrophys.*, 28, 219-229, 2014.



- Tang, J., Zhuang, Q., Shannon, R. D., and White, J. R.: Quantifying wetland methane emissions with process-based models of different complexities, *Biogeosciences*, 7, 3817-3837, 2010.
- Thomas, K. L., Benstead, J., Davies, K. L., and Lloyd, D.: Role of wetland plants in the diurnal control of CH<sub>4</sub> and CO<sub>2</sub> fluxes in peat, *Soil Biol. Biochem.*, 28(1), 17-23, 1996.
- 5 Tokida, T., Miyazaki, T., and Mizoguchi, M.: Ebullition of methane from peat with falling atmospheric pressure, *Geophys. Res. Lett.* 3232, L13823, doi:10.1029/2005GL022949, 2005.
- Tokida, T., Miyazaki, T., Mizoguchi, M., Nagata, O., Takakai, F., Kagemoto, A., and Hatano, R.: Falling atmospheric pressure as a trigger for methane ebullition from peatland, *Global Biogeochem. Cy.*, 21(2), doi: 10.1029/2006GB002790, 2007.
- Turetsky, M. R., Kotowska, A., Bubier, J., Dise, N. B., Crill, P., Hornibrook E. R. C., Minkinen, K., Moore, T. R., Myers-Smith, I. H., Nykänen, H., Olefeldt, D., Rinne, J., Saarnio, S., Shurpali, N., Tuittila, E.-S., Waddington, J. M., White, J. R., Wickland, K. P., and Wilking, M.: A synthesis of methane emissions from 71 northern, temperate, and subtropical wetlands, *Global Change Biology*, 20, 2183-2197, 2014.
- 10 Valentine, D. W., Holland, E. A., and Schimel, D. S.: Ecosystem and physiological controls over methane production in northern wetlands, *J. Geophys. Res.*, 99, 1563-1571, 1994.
- 15 van Huissteden, J., Petrescu, A. M. R., Hendriks, D. M. D., and Rebel, K. T.: Sensitivity analysis of a wetland methane emission model based on temperate and arctic wetland sites, *Biogeosciences*, 6, 3035-3051, 2009.
- Vile, D., Garnier, E., Shipley, B., Laurent, G., Navas, M.-L., Roumet, C., Lavorel, S., Diaz, S., Hodgson, J. G., Lloret, F., Midgley, G. F., Poorter, H., Rutherford, H., Wilson, P. J., and Wright I. J.: Specific leaf area and dry matter content estimate thickness in laminar leaves, *Ann. Bot.*, 96(6), 1129-1136, 2005.
- 20 Waddington, J. M., Roulet, N. T., and Swanson, R. V.: Water table control of CH<sub>4</sub> emission enhancement by vascular plants in boreal peatlands, *J. Geophys. Res., Atmospheres*, 101(D17), 22775-22785, 1996.
- Waddington, J.M., Harrison, K., Kellner, E., and Baird, A. J.: Effect of atmospheric pressure and temperature on entrapped gas content in peat, *Hydrol. Process.*, 23, 2970–2980, doi:10.1002/hyp.7412, 2009.
- Walter, B. P., Heimann, M., Shannon, R. D., and White, J. R.: A process-based model to derive methane emissions from natural wetlands, *Geophys. Res. Lett.*, 23(25), 3731-3734, 1996.
- 25 Walter, B. and Heimann, M.: A process-based climate-sensitive model to derive methane emissions from natural wetlands: Application to five wetland sites, sensitivity to model parameters, and climate, *Global Biogeochem. Cy.*, 14(3), 745-765, 2000.
- Wania, R., Ross, I., and Prentice, I. C.: Implementation and evaluation of a new methane model within a dynamic global vegetation model: LPJ-WHyMe v.1.3.1, *Geosci. Model Dev.*, 3, 565-584, 2010.
- 30 Watson, A., Stephen, K. D., Nedwell, D. B., and Arah, J. R. M.: Oxidation of methane in peat: Kinetics of CH<sub>4</sub> and O<sub>2</sub> removal and the role of plant roots, *Soil Biol. Biochem.*, 29(8), 1257-1267, 1997.
- Webb, E. K., Pearman, G. I., and Leuning, R.: Correction of flux measurements for density effects due to heat and water vapour transfer, *Q. J. R. Meteorol. Soc.*, 106, 85–100, 1980.



Whalen, S. C. and Reeburgh, W. S.: Moisture and temperature sensitivity of CH<sub>4</sub> oxidation in boreal soils, *Soil Biol. Biochem.*, 28(10/11), 1271-1281, 1996.

Whiting, G. J. and Chanton, J. P.: Primary production control of methane emission from wetlands, *Nature*, 364, 794-795, 1993.

Wilson, D., Alm, J., Riutta, T., Laine, J., Byrne, K. A., Farrell, E. P., and Tuittila, E.-S.: A high resolution green area index for  
5 modelling the seasonal dynamics of CO<sub>2</sub> exchange in peatland vascular plant communities, *Plant Ecol.*, 190, 37-51, 2007.

Xu, X., Yuan, F., Hanson, P. J., Wullschleger, S. D., Thornton, P. E., Riley, W. J., Song, X., Graham, D. E., Song, C., and  
Tian, H.: Reviews and syntheses: Four decades of modeling methane cycling in terrestrial ecosystems, *Biogeosciences*, 13,  
3735–3755, 2016.

Zhu, Q., Liu, J., Peng, C., Chen, H., Fang, X., Jiang, H., Yang, G., Zhu, D., Wang, W., and Zhou, X.: Modelling methane  
10 emissions from natural wetlands by development and application of the TRIPLEX-GHG model, *Geosci. Model Dev.*, 7, 981-  
999, 2014.

15

20

25

30



5 **Table 1: Model parameters and their values. We used for several parameters values that were obtained in a parallel study by Susiluoto et al. (2017, *in prep.*) in which HIMMELI was optimized for the Siikaneva measurement site.**

Symbol	Definition	Value	Reference
$\lambda$	decay length (in root distribution)	0.24	Susiluoto et al. (2017)
$f_m$	fraction of anaerobic respiration becoming methane	0.5 / 0.25*	- / Susiluoto et al. (2017)
$V_R$	potential rate of aerobic respiration at 10°C [mol m <sup>-3</sup> s <sup>-1</sup> ]	8.7x10 <sup>-5</sup>	Susiluoto et al. (2017)
$K_R$	Michaelis constant for aerobic respiration reaction [mol m <sup>-3</sup> ]	0.22	Arah and Stephen (1998)
$V_O$	potential oxidation rate at 10°C [mol m <sup>-3</sup> s <sup>-1</sup> ]	2.7x10 <sup>-4</sup>	Susiluoto et al. (2017)
$K_{O_2}$	Michaelis constant for O <sub>2</sub> in oxidation [mol m <sup>-3</sup> ]	0.33	Arah and Stephen (1998)
$K_{CH_4}$	Michaelis constant for CH <sub>4</sub> in oxidation [mol m <sup>-3</sup> ]	0.44	Arah and Stephen (1998)
$\Delta E_R$	activation energy of aerobic respiration [J mol <sup>-1</sup> ]	93000	Susiluoto et al. (2017)
$\Delta E_O$	activation energy of oxidation [J mol <sup>-1</sup> ]	49000	Susiluoto et al. (2017)
$T_\theta$	reference temperature for oxidation and aerobic respiration [K]	283	Arah and Stephen (1998)
$k$	time constant of ebullition [s <sup>-1</sup> ]	1/1800	This study
$a_{mA}$	root ending area per root dry biomass [m <sup>2</sup> kg <sup>-1</sup> ]	0.17	Susiluoto et al. (2017)
$\tau$	root tortuosity	1.0	Susiluoto et al. (2017)
SLA	specific leaf area of gas-transporting plants [m <sup>2</sup> kg]	23	Vile et al. (2005)
$f_{D,w}$	reduction factor for diffusion in water-filled peat	0.90	Susiluoto et al. (2017)
$f_{D,a}$	reduction factor for diffusion in air-filled peat	0.37	Susiluoto et al. (2017)
$\eta$	sensitivity of methanogenesis to oxygen [m <sup>3</sup> mol <sup>-1</sup> ]	400	Arah and Stephen (1998)
$\sigma$	peat porosity	0.85	Susiluoto et al. (2017)

\*The former value (0.5) was used in the steady-state tests and the latter (0.25) in the model runs on Siikaneva.



**Table 2: Summary of the steady-state sensitivity tests in which response of HIMMELI to different input combinations was analyzed.**

5

Test name	T (°C)	WTD (m)	LAI (m <sup>2</sup> m <sup>-2</sup> )	Anoxic respiration (μmol m <sup>-2</sup> s <sup>-1</sup> )
T_W0_L0_R1	0, 5, 10, 20, 25	0	0	1
T_W0_L1_R1	0, 5, 10, 20, 25	0	1	1
L_W0_T10_R1	10	0	0, 0.5, 1, 2, 3	1
L_W03_T10_R1	10	-0.3	0, 0.5, 1, 2, 3	1
W_L0_T10_R1	10	-0.5, -0.3, -0.2, -0.1, 0, 0.05	0	1
W_L1_T10_R1	10	-0.5, -0.3, -0.2, -0.1, 0, 0.05	1	1
R_W0_L0_T10	10	0	0	0.01, 0.1, 0.5, 1, 5, 10
R_W0_L1_T10	10	0	1	0.01, 0.1, 0.5, 1, 5, 10
R_W03_L0_T10	10	-0.3	0	0.01, 0.1, 0.5, 1, 5, 10
R_W03_L1_T10	10	-0.3	1	0.01, 0.1, 0.5, 1, 5, 10

10

15

20



**Table 3: Summary of the transition tests on model sensitivity to input data and the input combinations used in the tests.**

5

Test name	T (°C)	WTD (m)	LAI (m <sup>2</sup> m <sup>-2</sup> )	Anoxic respiration (μmol m <sup>-2</sup> s <sup>-1</sup> )
Wtr_L1	10	0, -0.2, -0.4, -0.2, 0	1	1
Wtr_L0	10	0, -0.2, -0.4, -0.2, 0	0	1
Rtr_W0_L1	10	0	1	1, 3, 6, 3, 1
Rtr_W0_L0	10	0	0	1, 3, 6, 3, 1

10

15

20

25



5 **Table 4: Results of the sensitivity testing. The rightmost column tells how much the CH<sub>4</sub> emissions changed when the input changed. The +/- signs in front of ‘Input change’ and ‘Change in CH<sub>4</sub> emission’ show the directions of change in input and the corresponding response in CH<sub>4</sub> emissions. This is expressed as % of potential CH<sub>4</sub> production (see Sect. 3.1.3) for the first 6 tests and as % of change in input anoxic respiration for the tests on changing input respiration. In some tests, the response was not constant over the input range. In that case, the result is also expressed as a range.**

Test	Changing input variable	Input change	Change in CH <sub>4</sub> emission, 10 % of potential production/ % of change in respiration	
T_W0_L0_R1	temperature	+1°	+0.02%	
T_W0_L1_R1	temperature	+1°	+1.4%	
L_W0_T10_R1	LAI	+0.1 m	-0.4%...11%	15
L_W03_T10_R1	LAI	+0.1 m	-1.2%	
W_L0_T10_R1	WTD	-0.05 m	-0.02%...2%	
W_L1_T10_R1	WTD	-0.05 m	+0.5%...10%	
R_W0_L0_T10	respiration	+	+99%...100%	
R_W0_L1_T10	respiration	+	+22%...80%	20
R_W03_L0_T10	respiration	+	+88%...93%	
R_W03_L1_T10	respiration	+	+43%...92%	

25

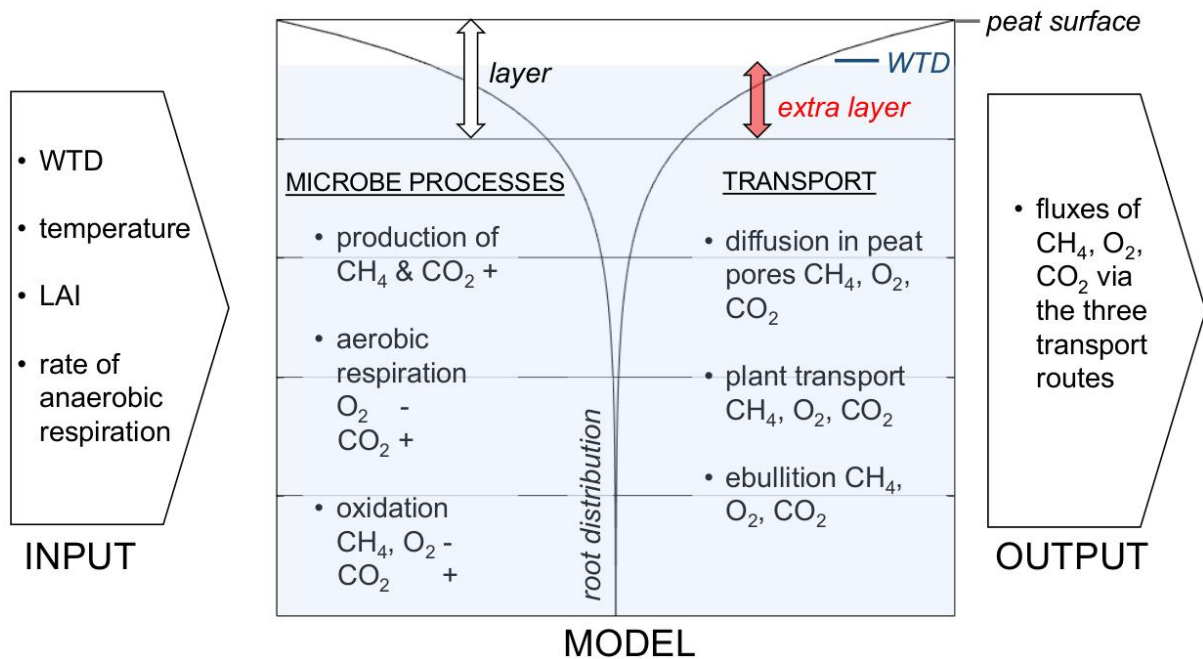
30

35



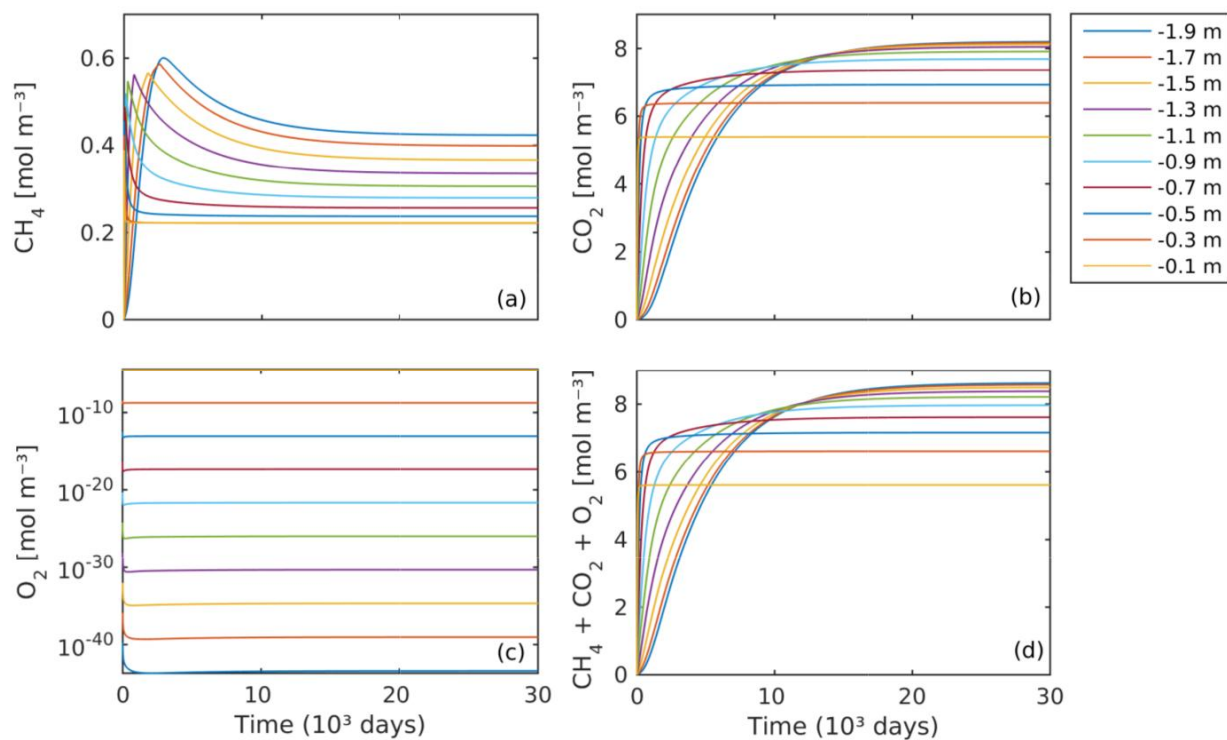
5 **Table B1: Parameter values of the models used for producing input for the Siikaneva runs. Values marked with asterisk (\*) base on the study Susiluoto et al. (2017), the others are from the original references of the photosynthesis and respiration models.**

Symbol	Definition	Value
$P_{max}$	maximum potential CO <sub>2</sub> uptake [mol (C) s <sup>-1</sup> m <sup>-2</sup> ground area]	1.24x10 <sup>-5</sup>
$k$	PAR at which half of maximum photosynthesis is reached [μmol m <sup>-2</sup> s <sup>-1</sup> ]	223.9
$a$	initial slope of saturating leaf-area response function	0.778
$T_{opt}$	optimal air temperature [°C]	24.88
$T_{tol}$	temperature tolerance [°C]	14.69
$d_{W,opt}$	optimal water table depth [cm]	-29.1
$d_{W,tol}$	water table depth tolerance [cm]	67.27
$R_{ref}$	respiration rate in reference conditions [mol (C) s <sup>-1</sup> m <sup>-2</sup> leaf area]	6.94x10 <sup>-7</sup>
$b$	activation energy/gas constant [K]	300
$T_{ref}$	reference temperature of autotrophic respiration [K]	283.15
$T_0$	T at which R = 0 [K]	227.13
$LAI_{max}$	peak LAI	0.4
$LAI_{min}$	overwintering LAI	0.05
$j_{max}$	Julian date of the peak LAI	209
$c$	parameter to adjust the LAI curve shape	0.2
$f_{exu}$	fraction of NPP converted to root exudates	0.4*
$R_{ref,pR}$	reference temperature of peat respiration [K]	273.15
$Q_{10}$	base value for temperature dependence of peat respiration	4.6*
$\tau_C$	turnover time of the catotelm carbon pool [y]	14700*
$\rho_C$	density of the carbon pool [mol (C) m <sup>-3</sup> ]	3940



5 **Figure 1. HIMMELI as a simplified schematic picture. The microbial and transport processes are simulated in a vertically layered one-dimensional peat column in which roots of aerenchymatous gas-transporting plants are distributed according to the exponential root distribution function. The input anoxic respiration is distributed along the root distribution. Input water table depth (WTD) determines the thickness of the possible extra layer that is introduced in case the WTD does not match any of the fixed background layer borders. This ensures that all the simulated layers are either completely water-filled or air-filled. The + sign shows that the compound is produced in the microbial process and – sign means consumption of the compound.**

10

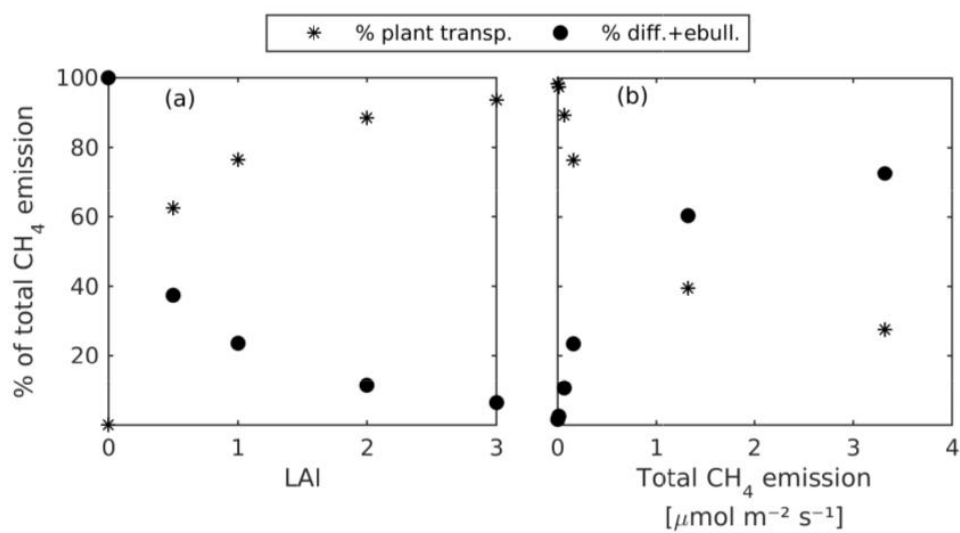


5

**Figure 2.** Evolution of the concentration profiles of (a)  $\text{CH}_4$ , (b)  $\text{CO}_2$  (c)  $\text{O}_2$  and (d) their sum in a simulation where both WTD and LAI were zero, i.e., there was no plant transport of these compounds. Different colors show the concentrations at different depths in the peat. In the beginning of the simulation, all the concentrations were zero.

10

15

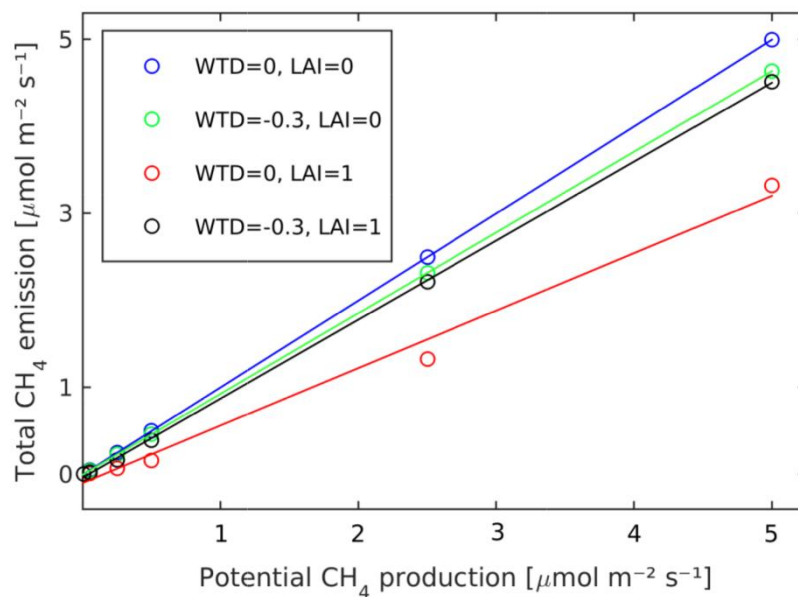


5

Figure 3. Contribution of different transport routes to the total CH<sub>4</sub> emission (a) as a function of LAI in test L\_W0\_T10\_R1 and (b) as a function of total CH<sub>4</sub> emission in test R\_W0\_L1\_T10.

10

15

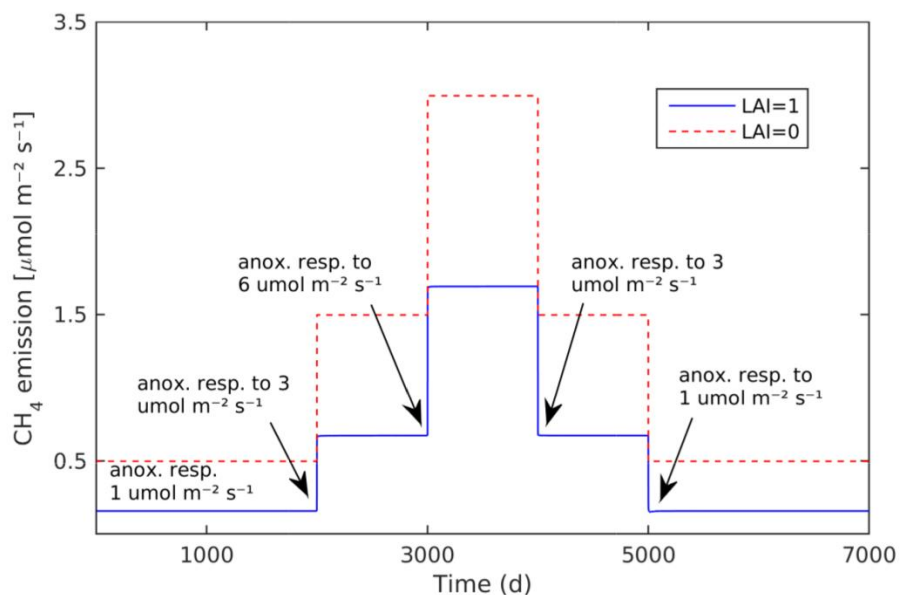


5

Figure 4. Dependence of the total output CH<sub>4</sub> emission on the potential CH<sub>4</sub> production rate in tests on the model sensitivity to input anoxic respiration, i.e. tests that were named starting with R\_.

10

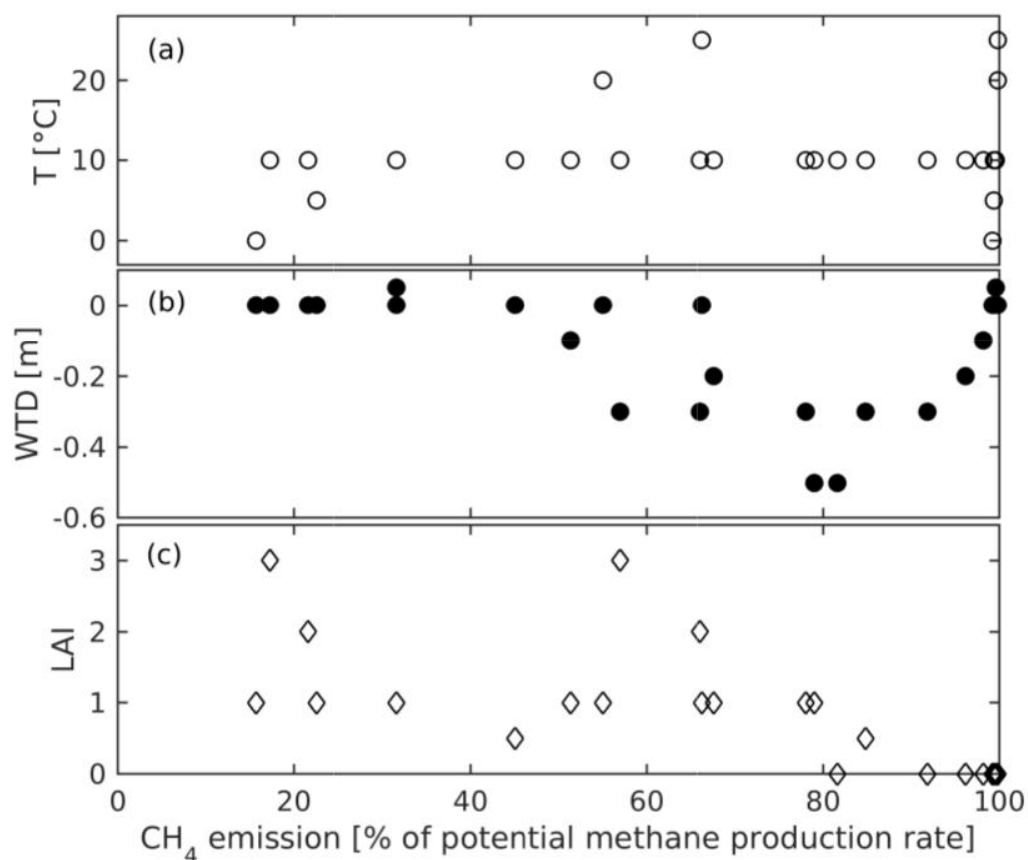
15



5 **Figure 5. Output CH<sub>4</sub> emission responded clearly to changes in the input anoxic respiration rate in the transition tests Rtr\_W0\_L1 (blue line) and Rtr\_W0\_L0 (red dashed line) (see Table 3). Black arrows indicate when the input changed.**

10

15



5 **Figure 6.** Relationship between the relative CH<sub>4</sub> emission rate (expressed as % of potential CH<sub>4</sub> production) and different combinations of input (a) temperature, (b) WTD and (c) LAI in the steady-state sensitivity tests with constant anoxic respiration (test names ending with \_R1).

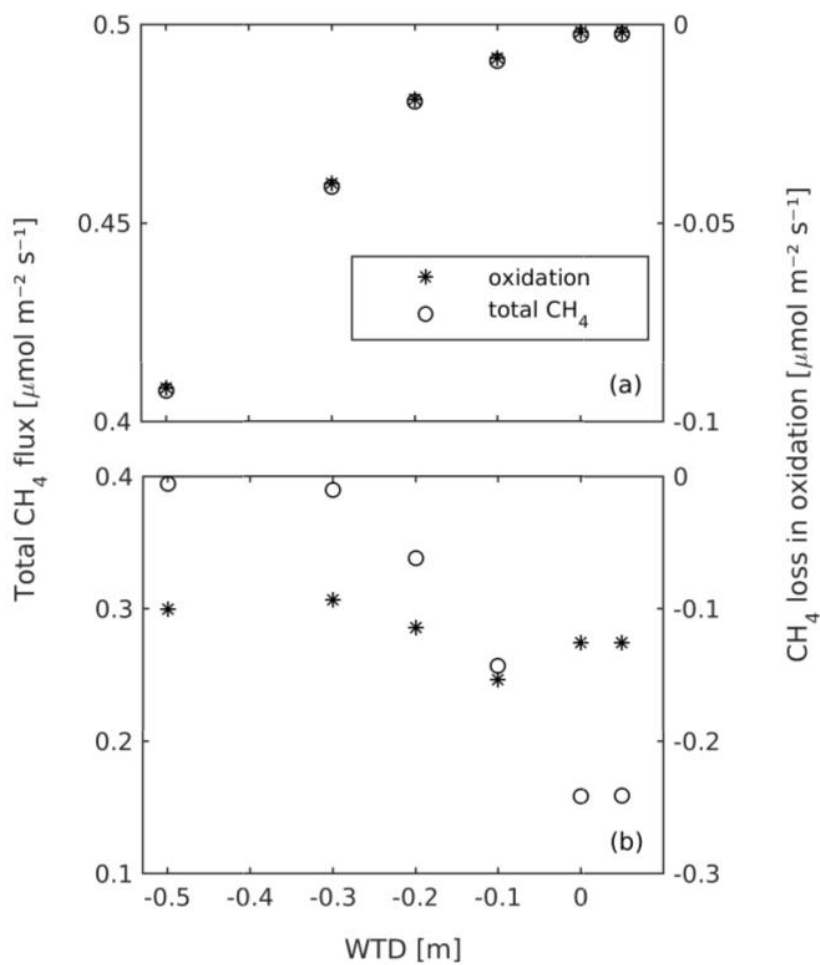
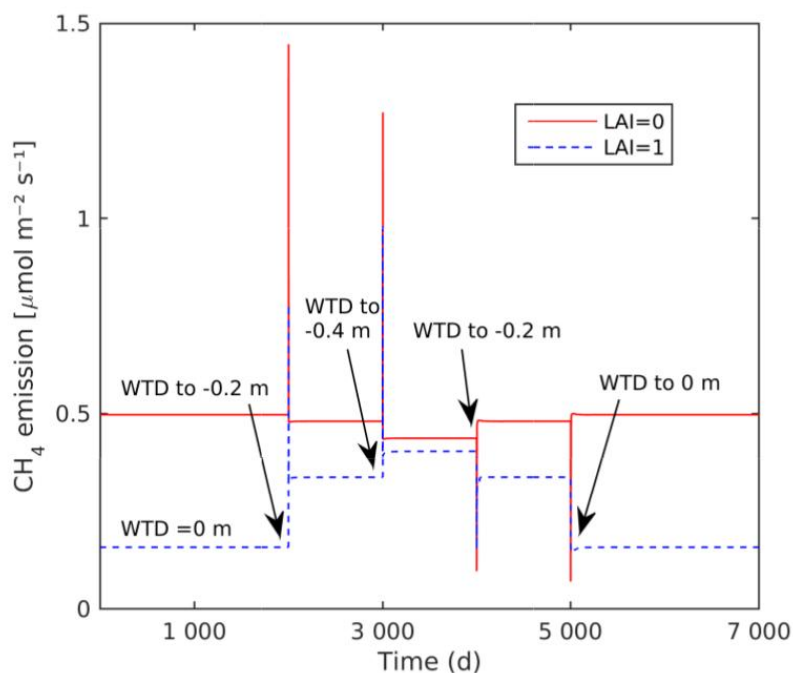


Figure 7. Dependence of the total CH<sub>4</sub> flux and CH<sub>4</sub> oxidation rate on WTD in (a) test W\_L0\_T10\_R1 and (b) test W\_L1\_T10\_R1. CH<sub>4</sub> oxidation is a negative flux since it is loss of CH<sub>4</sub>.

5

10



5 **Figure 8. Effect of abrupt changes in WTD on the total output CH<sub>4</sub> emissions in transition tests Wtr\_L0 (red line) and Wtr\_L1 (blue dashed line). Black arrows indicate the change in WTD. This figure also shows how changes in the WTD cause a short artefact peak in the flux, because of how the CH<sub>4</sub> (and CO<sub>2</sub> and O<sub>2</sub>) in layers receiving or losing water is handled in the model (see Sect. 3.1.2).**

10

15

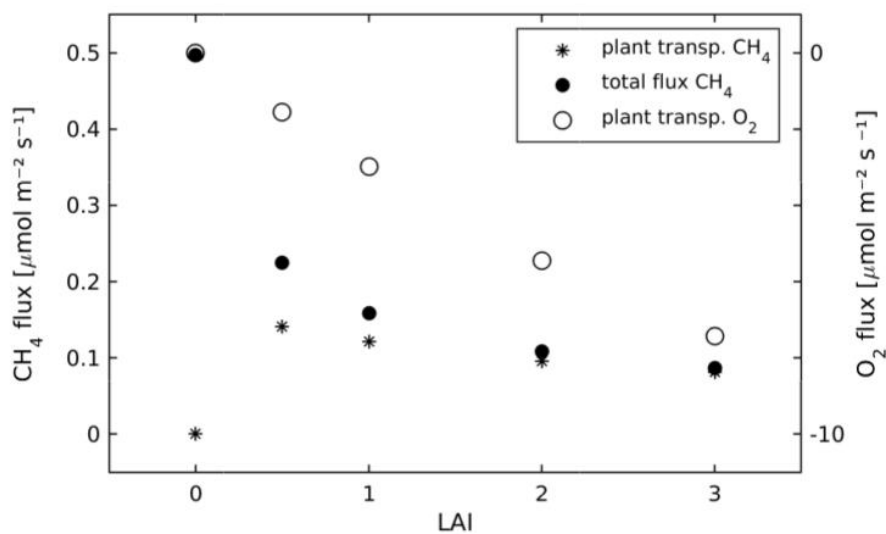
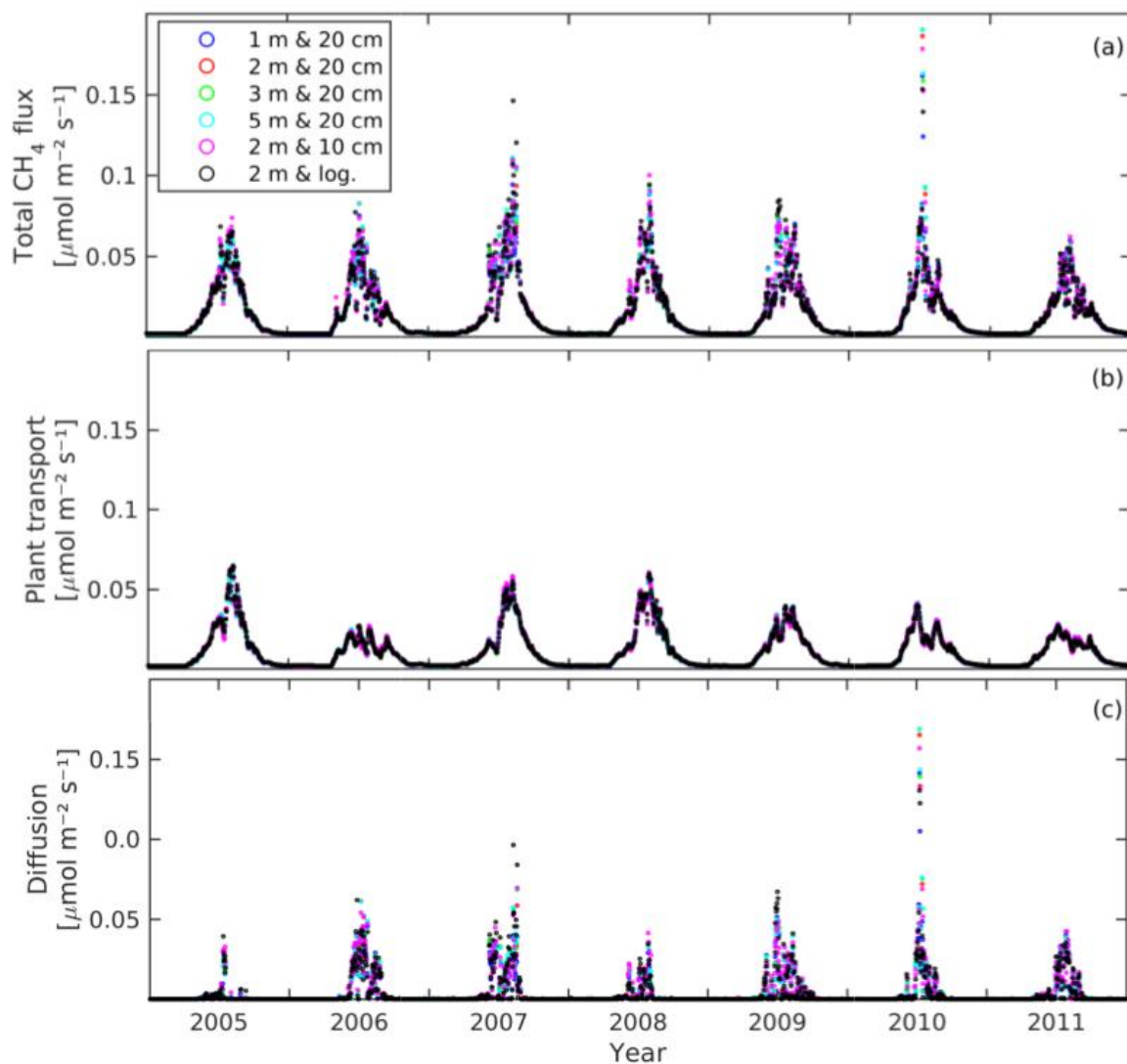
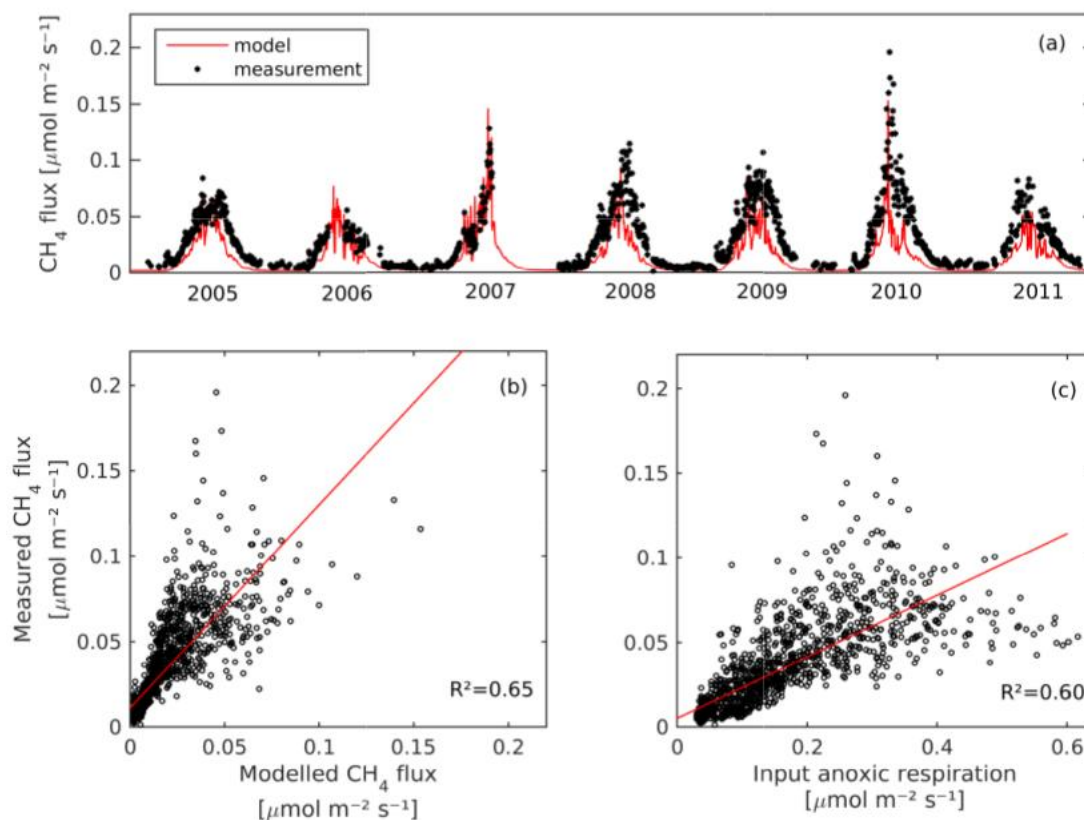


Figure 9. Dependence of total and plant-transported fluxes of CH<sub>4</sub> and plant transport of O<sub>2</sub> on LAI in test L\_W0\_T10\_R1.



5 Figure 10. Time series of CH<sub>4</sub> fluxes simulated for Siikaneva in 2005...2011, using different peat depths and layer thicknesses with the same input anoxic respiration rate. (a) Total CH<sub>4</sub> flux, (b) plant transport, (c) diffusion. Direct ebullition to the atmosphere was negligible and thus not shown. CH<sub>4</sub> ebullited when WTD was below the peat surface was transported to the atmosphere via diffusion in peat or plant roots.



5 **Figure 11.** Comparison of the measured and modelled CH<sub>4</sub> fluxes of Siikaneva. The modelled flux is from the simulation with logarithmic layer structure and 2 m of peat, driven with measured temperature profile and WTD and simulated LAI and anoxic respiration. (a) The time series of measurements versus model, (b) correlation between model and measurement, (c) correlation between the anoxic respiration rate given as input to the model and the measured CH<sub>4</sub> fluxes.